Review Article

State of the Art of UV/Chlorine Advanced Oxidation Processes: Their Mechanism, Byproducts Formation, Process Variation, and Applications

Naoyuki Kishimoto

Faculty of Science and Technology, Ryukoku University, Otsu, Japan

ABSTRACT

The photolysis of chlorine by ultraviolet radiation (UV/chlorine) produces HO· and Cl·, part of which further transforms into reactive chlorine species (RCS) like $Cl_2^{·-}$ and ClO·. These radicals are responsible for the advanced oxidation effect of UV/chlorine processes. Recently, UV/chlorine processes gather much attention from researchers and practitioners and published papers on UV/chlorine processes have drastically increased, which were thoroughly reviewed in this paper for understanding the state of the art of these technologies. Fundamental studies elucidate that acidic conditions are favorable to UV/chlorine processes through a change in quantum yield of chlorine photolysis, equilibrium shifts of radical species, and a change in radical scavenger effect of free chlorine. Comparative studies reveal that UV/chlorine processes are usually more energy-efficient than UV/hydrogen peroxide and UV/persulfate processes. Although unfavorable byproducts formation by RCS reactions is apprehended, application researches in real waters show that UV/chlorine processes do not enhance disinfection byproducts formation very much. Since UV irradiation and chlorination are widely used unit operations, a barrier to install an UV/chlorine process into a conventional process is not high. It is desired to develop and optimize a whole process combined with other unit processes for maximizing benefits in water treatment in the future.

Keywords: advanced oxidation technology, chlorine photolysis, disinfection byproducts, hydroxyl radical, reactive chlorine species

CONTENTS

Corresponding author: Naoyuki Kishimoto, E-mail: naoyuki@rins.ryukoku.ac.jp

Open Access This is an open-access article distributed under the terms of the Creative Commons Attribution (CC BY) 4.0 License. http://creativecommons.org/licenses/by/4.0/

INTRODUCTION

Chemicals registered in Chemical Abstract Service (CAS) of American Chemical Society have increased exponentially and reached over 100 million in 2015. These chemicals support our convenient and comfortable life. However, parts of chemicals are toxic and registered for aggregating their release to the environment. For instance, Japanese government built a pollutant release and transfer register (PRTR) system in 2001, in which 462 chemicals are registered (checked on January 12th, 2019). Organic chemicals registered in the PRTR system contain biochemically and/or chemically persistent ones, which are difficult to be efficiently removed from water streams by conventional wastewater treatment processes like activated sludge processes and coagulation processes.

Advanced oxidation processes (AOPs) were firstly defined by Glaze *et al.* as processes involving the generation of hydroxyl radicals (HO˙) in sufficient quantity to affect water purification [1]. But, nowadays the word "AOPs" is widely used as chemical oxidation processes using strong oxidants of sulfate radical (SO$_4$˙⁻), chlorine atom (Cl˙), and so on in addition to HO˙. According to strong oxidants AOPs are promising processes for degrading biochemically and/or chemically persistent organic compounds. There are many kinds of AOPs proposed. Among them, the Fenton process, ozone-based AOPs like ozonation with hydrogen peroxide addition (O$_3$/H$_2$O$_2$), and ultraviolet (UV) irradiation-based AOPs like UV photolysis of hydrogen peroxide (UV/H$_2$O$_2$) are the most popular in practical applications [2]. Although AOPs are effective in eliminating persistent organic pollutants, they also have a few disadvantages of plenty of iron sludge generation in the Fenton process, higher investment of ozonizer and peripheral equipment, higher chemical cost of hydrogen peroxide, etc.

Recently, UV photolysis of chlorine (UV/chlorine) gathers much attention from researchers and practitioners as a new AOP. UV/chlorine AOPs involve unit processes of chlorination and UV irradiation, which are the most popular disinfection processes. Therefore, UV/chlorine AOPs have an
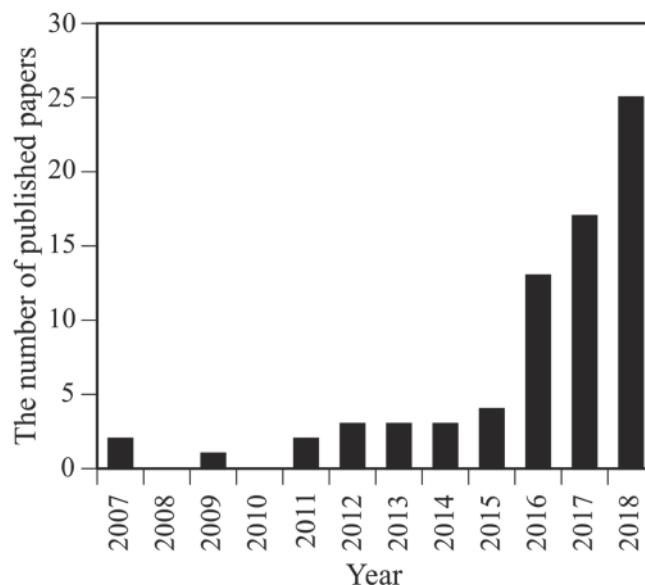

Fig. 1 The number of published papers on UV/chlorine AOPs every year. Papers related to UV/chlorine AOPs were manually picked up from journal articles found in SCOPUS database with search words of "UV", "chlorine", and "advanced oxidation". The database was accessed on January 12th, 2019.

advantage of easy installation into conventional processes, because the technical know-how of managing chlorination and UV irradiation facilities has been already established. Two hundred and eighteen journal articles were found from the SCOPUS database with search words of "UV", "chlorine", and "advanced oxidation" (accessed on January 12th, 2019). After papers not related to UV/chlorine AOPs were omitted manually from the found articles, 77 papers finally remained. The number of papers published every year is summarized in **Fig. 1**. This figure clearly shows that the number of papers on UV/chlorine AOPs rapidly increased from 2016. Thus, UV/chlorine processes are new AOPs and scientific and technical knowledge has been rapidly accumulated in late years. In this paper published articles related to UV/chlorine AOPs are thoroughly reviewed for elucidating the state of the art of these technologies.

ADVANCED OXIDATION MECHANISM

Photolysis of chlorine

Greenish-yellow fumes of chlorine had been already known in the 13th century, though the name of "chlorine" was proposed by Davy in the early 19th century [3]. The bleaching properties of chlorine were intensively studied
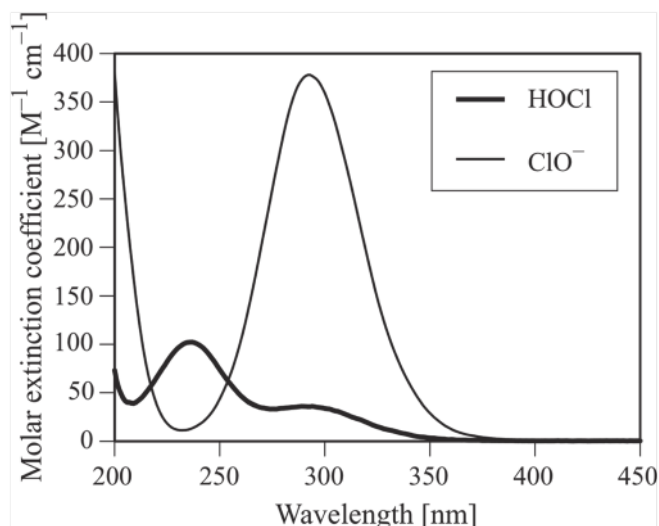
Fig. 2 Absorption spectra of HOCl and ClO$^-$.

by Berthollet in the late 18th century [3]. He also found that light irradiation to chlorine water produced oxygen and hydrochloric acid [4]. **Figure 2** shows absorption spectra of hypochlorous acid (HOCl) and hypochlorite ion (ClO$^-$) [5]. Absorption bands of both species are in the range of UV region, but are quite different each other; HOCl has two absorption peaks at 237 nm with molar extinction coefficient (ε) of 102 M^{-1} cm^{-1} and 289 nm with ε of 36.1 M^{-1} cm^{-1}, whereas ClO$^-$ has a strong absorption peak at 292 nm with ε of 378 M^{-1} cm^{-1} and does not show strong absorption around 230 nm. Thus, UV light is preferable for photolysis of chlorine. After Peter Cooper Hewitt invented a low-pressure mercury lamp in 1900 [6] many papers have been published on photolysis of chlorine using Cooper-Hewitt quartz mercury lamps. Interestingly, the ε of HOCl at the emission line of low-pressure mercury vapor lamp like Cooper-Hewitt quartz mercury lamp almost accords with that of ClO$^-$; namely 62 M^{-1} cm^{-1} at 254 nm. Allmand et al. discussed the photochemical reaction of chlorine water in a systematic fashion using a Cooper-Hewitt lamp and proposed that HOCl were photolyzed into hydrochloric acid and oxygen atom [7,8]. However, this photochemical reaction was revised in a follow-up paper as follows [9]:
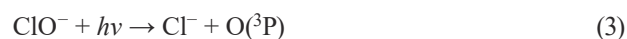
$$HOCl + h\nu \rightarrow HO^\cdot + Cl^\cdot - 55 \text{ kcal} \tag{1}$$
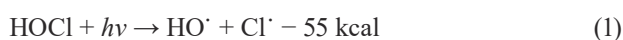
Thomsen, Madsen, and co-workers investigated femtosecond photolysis of HOCl at 250–330 nm and confirmed the reaction (1) [10,11]. They mentioned that the O–H bond length in HOCl is very close to that in HO$^\cdot$ and consequently photolysis of HOCl by UV light below 340 nm produces HO$^\cdot$

+ Cl$^\cdot$. Thus, the molar yield of active radicals, namely HO$^\cdot$ and Cl$^\cdot$ in the photolysis of HOCl is 2 mol-active radicals/mol-HOCl.

In ClO$^-$ Young and Allmand suggested a following photochemical reaction [9].

$$ClO^- + H_2O + h\nu \rightarrow HO^\cdot + Cl^\cdot + OH^- - 64 \text{ kcal} \tag{2}$$

Buxton and Subhani investigated the photolysis of ClO$^-$ carefully by flash photolysis techniques and identified the following photochemical reactions [12].

$$ClO^- + h\nu \rightarrow Cl^- + O(^3P) \tag{3}$$

$$ClO^- + h\nu \rightarrow Cl^\cdot + O^{\cdot-} \tag{4}$$

$$ClO^- + h\nu \rightarrow Cl^- + O(^1D) \tag{5}$$

They observed that the reactions (3) and (4) were primary reactions at 365 nm, whereas the quantum yield of reaction (3) was 3.5 times higher than that of reaction (4). In contrast, three reactions were significant below 320 nm; the quantum yield ratio of reactions (3), (4), and (5) was 1.0:1.7:0.27 at 313 nm and 1.0:3.8:1.8 at 253.7 nm, respectively. Active oxygen species of oxygen anion radical (O$^{\cdot-}$) and singlet oxygen (O (^1D)) take part in the following reactions.

$$O^{\cdot-} + H_2O \leftrightarrow HO^\cdot + OH^- \tag{6}$$

$$O(^1D) + H_2O \rightarrow H_2O_2 \tag{7}$$
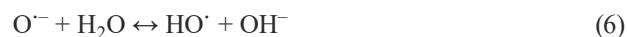
Since hydrogen peroxide (H$_2$O$_2$) is further photolyzed and produces two HO$^\cdot$ [13], the photolysis of ClO$^-$ through reactions (4) and (5) is proved to produce two active radicals; 2HO$^\cdot$ or HO$^\cdot$ + Cl$^\cdot$. According to these chain reactions, the reaction (2) is proved to be an overall reaction of reactions (4) and (6). When a solution contains dissolved oxygen (O$_2$), triplet oxygen (O (^3P)) reacts with O$_2$ and produces ozone (O$_3$) [12].

$$O(^3P) + O_2 \rightarrow O_3 \tag{8}$$

Since UV photolysis of O$_3$ produces two HO$^\cdot$ through photochemically produced H$_2$O$_2$ [14], the photochemical reaction (3) followed by reaction (8) also produces two HO$^\cdot$ from ClO$^-$. However, O (^3P) also reacts with excess ClO$^-$ as follows [12]:

$$O(^3P) + ClO^- \rightarrow ClO_2^- \tag{9}$$

Therefore, the overall molar yield of active radical species will be lower than 2 mol-active radicals/mol-ClO$^-$, especially at the UV light above 320 nm.
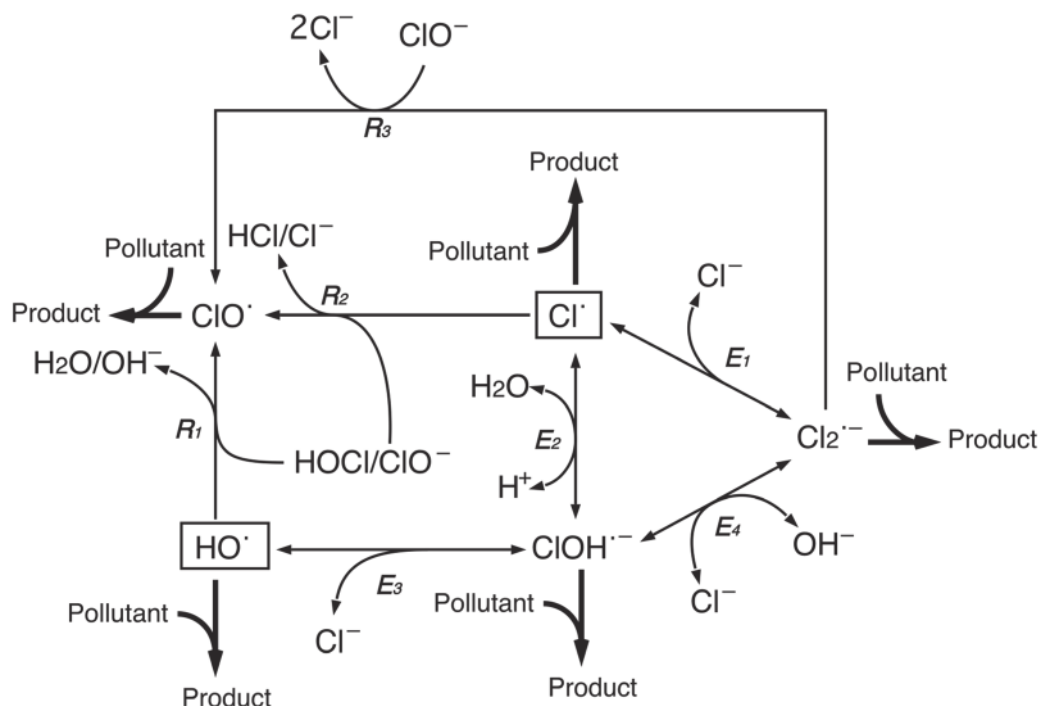
Fig. 3 Radical reaction scheme in UV/chlorine AOPs. The original figure in reference [19] is partially revised. Boxes depict primary radicals produced by photolysis of chlorine.

Reactive radical species

As described in "Photolysis of chlorine" section, primary radicals in UV/chlorine AOPs are HO$^{\cdot}$ and Cl$^{\cdot}$. The former has standard electrode potentials of 2.73 V vs. NHE (normal hydrogen electrode) in acid and 1.90 V vs. NHE in alkali, and the latter has a standard electrode potential of 2.20–2.60 V vs. NHE [15]. Thus, both radicals are strong oxidants. However, HO$^{\cdot}$ and Cl$^{\cdot}$ react with excess free chlorine and chloride ion (Cl^{-}), and produce secondary radicals of chlorine oxide radical (ClO$^{\cdot}$), chloro-hydroxide anion radical (ClOH$^{\cdot-}$), and dichlorine radical (Cl$_2^{\cdot-}$) [16], whose standard electrode potentials are 1.41–1.8, 1.90, 2.09–2.30 V vs. NHE, respectively [15,17,18]. An example of radical reaction scheme in UV/chlorine AOPs is depicted in **Fig. 3** and related reactions are listed in **Table 1** [19]. Although the standard electrode potential of ClO$^{\cdot}$ is lower than others, the chlorine derivative radicals of Cl$^{\cdot}$, ClO$^{\cdot}$, ClOH$^{\cdot-}$, Cl$_2^{\cdot-}$, etc. are called "reactive chlorine species (RCS)" that are also responsible for advanced oxidation by UV/chlorine processes [20–23]. However, the reactivity of each radical species is thought to be different from others. Therefore, it is important to elucidate the reactivity of each radical species with chemical compounds for understanding the efficacy of UV/chlorine AOPs.

Table 2 summarizes reaction rate constants of HO$^{\cdot}$, Cl$^{\cdot}$, ClO$^{\cdot}$, and Cl$_2^{\cdot-}$ with some chemicals reported in literatures [18,24–32]. HO$^{\cdot}$ has second-order reaction rate constants with approximately 10^9-order level regardless of saturated compounds or benzene derivatives. Cl$^{\cdot}$ shows also high reaction rate constants coequal to HO$^{\cdot}$ except 1,4-dioxane, acetone, and nitrobenzene. ClO$^{\cdot}$ and Cl$_2^{\cdot-}$ slowly react with saturated compounds of alcohol, ketone, and carboxylic acid with 10^6-order rate constants or below. On the contrary, the RCS, especially ClO$^{\cdot}$, react with benzene derivatives more rapidly with 10^6-order or higher rate constants than saturated compounds. Thus, the RCS seem to be selective oxidants favorable to aromatic compounds. Among benzene derivatives, nitrobenzene particularly shows low reactivity with RCS. **Figure 4** shows Löwdin charge of each carbon in benzene derivatives, which were calculated by ab initio method with GAMESS (18Aug2016R1) [33]. When nitro group is added to benzene, charges of carbons in aromatic ring are shifted toward positive side. Since HO$^{\cdot}$ and RCS act as electrophilic reagents, the positive shift of carbon charge by nitro group addition is thought to be one of reasons of the less reactivity of nitrobenzene with RCS. Guo *et al*. studied the degradation of 34 pharmaceuticals and personal care products (PPCPs) by an UV/chlorine AOP and also stated

Table 1 Primary reactions in the UV/chlorine system.

Symbol	Reaction	Rate constant k, equilibrium constant K, or quantum yield φ	Reference
R_1	$HO^{\bullet} + ClO^- \rightarrow ClO^{\bullet} + OH^-$	$k_1 = 8.8\times10^9$ M^{-1} s^{-1}	[24]
	$HO^{\bullet} + HOCl \rightarrow ClO^{\bullet} + H_2O$	$k_{1H} = 8.46\times10^4$ M^{-1} s^{-1}	[29]
R_2	$Cl^{\bullet} + ClO^- \rightarrow ClO^{\bullet} + Cl^-$	$k_2 = 8.2\times10^9$ M^{-1} s^{-1}	[88]
	$Cl^{\bullet} + HOCl \rightarrow ClO^{\bullet} + H^+ + Cl^-$	$k_{2H} = 3.0\times10^9$ M^{-1} s^{-1}	[88]
R_3	$Cl_2^{\bullet-} + ClO^- \rightarrow ClO^{\bullet} + 2Cl^-$	$k_3 = 1.1\times10^8$ M^{-1} s^{-1}	[132]
E_1	$Cl^{\bullet} + Cl^- \leftrightarrow Cl_2^{\bullet-}$	$K_1 = 1.9\times10^5$ M^{-1}	[133]
	$(Cl^{\bullet} + Cl^- \rightarrow Cl_2^{\bullet-})$	$k_{E1F} = 2.1\times10^{10}$ M^{-1} s^{-1}	[133]
	$(Cl_2^{\bullet-} \rightarrow Cl^{\bullet} + Cl^-)$	$k_{E1B} = 1.1\times10^5$ M^{-1} s^{-1}	[133]
E_2	$ClOH^{\bullet-} + H^+ \leftrightarrow Cl^{\bullet} + H_2O$	$K_2 = 2.9\times10^5$ M^{-1}	
	$(ClOH^{\bullet-} + H^+ \rightarrow Cl^{\bullet} + H_2O)$	$k_{E2F} = 2.1\times10^{10}$ M^{-1} s^{-1}	[133]
	$(Cl^{\bullet} + H_2O \rightarrow ClOH^{\bullet-} + H^+)$	$k_{E2B} = 7.2\times10^4$ s^{-1} [a]	[133]
E_3	$HO^{\bullet} + Cl^- \leftrightarrow ClOH^{\bullet-}$	$K_3 = 0.70$ M^{-1}	
	$(HO^{\bullet} + Cl^- \rightarrow ClOH^{\bullet-})$	$k_{E3F} = 4.3\times10^9$ M^{-1} s^{-1}	[133]
	$(ClOH^{\bullet-} \rightarrow HO^{\bullet} + Cl^-)$	$k_{E3B} = 6.1\times10^9$ s^{-1}	[133]
E_4	$Cl_2^{\bullet-} + OH^- \leftrightarrow ClOH^{\bullet-} + Cl^-$	$K_4 = 4.5\times10^3$	
	$(Cl_2^{\bullet-} + OH^- \rightarrow ClOH^{\bullet-} + Cl^-)$	$k_{E4F} = 4.5\times10^7$ M^{-1} s^{-1}	[89]
	$(ClOH^{\bullet-} + Cl^- \rightarrow Cl_2^{\bullet-} + OH^-)$	$k_{E4B} = 1.0\times10^4$ M^{-1} s^{-1}	[89]
R_{C1}	$ClO^{\bullet} + HO^{\bullet} \rightarrow ClO_2^- + H^+$	$k_{C1} > 1\times10^9$ M^{-1} s^{-1}	[134]
R_{C2}	$ClO_2^- + HO^{\bullet} \rightarrow ClO_2^{\bullet} + OH^-$	$k_{C2} = 6.3\times10^9$ M^{-1} s^{-1}	[135]
R_{C3}	$ClO_2^{\bullet} + HO^{\bullet} \rightarrow ClO_3^- + H^+$	$k_{C3} = 4\times10^9$ M^{-1} s^{-1}	[134]
R_{C4}	$ClO_3^- + HO^{\bullet} \rightarrow ClO_3^{\bullet} + OH^-$	$k_{C4} < 10^6$ M^{-1} s^{-1}	[135]
R_{C5}	$ClO_2^- + Cl_2^{\bullet-} \rightarrow ClO_2^{\bullet} + 2Cl^-$	$k_{C5} = 2.05\times10^8$ M^{-1} s^{-1} [b]	[132]
R_{C6}	$ClO_3^- + Cl^{\bullet} \rightarrow ClO_3^{\bullet} + Cl^-$	$k_{C6} < 10^6$ M^{-1} s^{-1}	[45,124]
R_{C7}	$ClO_2^- + ClO^{\bullet} \rightarrow ClO^- + ClO_2^{\bullet}$	$k_{C7} = 9.4\times10^8$ M^{-1} s^{-1}	[124]
R_{C8}	$2ClO^{\bullet} \rightarrow Cl_2O_2$	$k_{C8} = 7.5\times10^9$ M^{-1} s^{-1}	[135]
R_{C9}	$Cl_2O_2 + H_2O \rightarrow ClO^- + O_2 + 2H^+ + Cl^-$	$k_{C9} = 93$ M^{-1} s^{-1}	[12,124]
R_{C10}	$Cl_2O_2 + H_2O \rightarrow ClO^- + ClO_2^- + 2H^+$	$k_{C10} = 180$ M^{-1} s^{-1}	[12,124]
R_{C11}	$2ClO^- \rightarrow ClO_2^- + Cl^-$	$k_{C11} = 10.75\times10^{-5}$ M^{-1} s^{-1} [c]	[136]
R_{C12}	$ClO^- + ClO_2^- \rightarrow ClO_3^- + Cl^-$	$k_{C12} = 4.41\times10^9$ M^{-1} s^{-1} [d]	[42]
R_{C13}	$2HOCl + ClO^- \rightarrow ClO_3^- + 2H^+ + 2Cl^-$	$k_{C13} = 0.0125$ M^{-2} s^{-2}	[42]
R_{C14} [e]	$2ClO_2^{\bullet} + 2OH^- \rightarrow ClO_2^- + ClO_3^- + H_2O$	$-$	[137]
	$4ClO_2^{\bullet} + 4OH^- \rightarrow 4ClO_2^- + O_2 + 2H_2O$	$-$	[137]
R_{C15}	$ClO_3^{\bullet} + HO^{\bullet} \rightarrow ClO_4^- + H^+$	$-$	[43]
R_{C16}	$ClO_3^{\bullet} + ClO^{\bullet} \rightarrow Cl_2O_4$	$k_{C16} = 7.5\times10^9$ M^{-1} s^{-1}	[138]
R_{C17}	$2ClO_3^{\bullet} \rightarrow Cl_2O_6$	$k_{C17} = 3.7\times10^9$ M^{-1} s^{-1}	[138]
R_{C18}	$Cl_2O_4 + H_2O \rightarrow ClO_4^- + ClO^- + 2H^+$	$k_{C18} = 180$ M^{-1} s^{-1}	[138]
R_{C19}	$Cl_2O_6 + H_2O \rightarrow ClO_4^- + ClO_3^- + 2H^+$	$k_{C19} = 180$ M^{-1} s^{-1}	[138]
R_{P1}	$ClO_2^- + h\nu \rightarrow ClO^{\bullet} + O^{\bullet-}$	$-$	[139]
R_{P2}	$ClO_2^- + h\nu \rightarrow ClO^- + O (^1D$ or $^3P)$	$-$	[44]
R_{P3}	$ClO_3^- + h\nu \rightarrow ClO_2^{\bullet} + O^{\bullet-}$	$-$	[140]
R_{P4}	$ClO_3^- + h\nu \rightarrow ClO_2^- + O (^3P)$	$-$	[140]
R_{P5}	$ClO_2^{\bullet} + h\nu \rightarrow ClO^{\bullet} + O (^1D$ or $^3P)$	$\varphi_{P5} / \varphi_{P6} = 9.0$	[44]
R_{P6}	$ClO_2^{\bullet} + h\nu \rightarrow Cl^{\bullet} + O_2$	$\varphi_{P5} / \varphi_{P6} = 9.0$	[44]
R_{P7}	$Cl_2O_2 + h\nu \rightarrow Cl^{\bullet} + ClO_2^{\bullet}$	$-$	[44]

[a] The original rate constant of 1.3×10^3 M^{-1} s^{-1} was converted by multiplying H_2O concentration of 55.6 M.
[b] Average of two values
[c] at 60°C
[d] The rate constant was pH-dependent. This value was estimated at pH 9.60.
[e] These are overall reactions. See the reference in detail.

Table 2 Second-order reaction rate constants of HO·, Cl·, ClO·, and $Cl_2^{·-}$ with organic chemicals [M^{-1} s^{-1}].

Chemical	HO·	Cl·	ClO·	$Cl_2^{·-}$
Alcohol	$9.7×10^8$ [24]	$1.0×10^9$ [32]	–	$3.5×10^3$ [25]
methanol	$1.9×10^9$ [24]	$1.7×10^9$ [32]	–	$4.5×10^4$ [25]
ethanol	$1.9×10^9$ [24]	$1.5–3.2×10^9$ [30]	–	$1.2–1.9×10^5$ [25]
2-propanol	$6.0×10^8$ [24]	$6.2×10^8$ [32]	$1.3×10^7$ [31]	0 [26]
t-butanol				
Aldehyde	$1.0×10^9$ [24]	$1.4×10^9$ [32]	–	$3.6×10^4$ [32]
formaldehyde				
Ether	$3.1×10^9$ [27]	$4.4×10^6$ [27]	–	$3.3×10^6$ [27]
1,4-dioxane				
Ketone	$1.1×10^8$ [24]	$<5.0×10^6$ [32]	–	$1.4×10^3$ [25]
acetone				
Carboxylic acid	$3.2×10^9$ [24]	$4.2×10^9$ [32]	$<1×10^6$ [18]	$1.9×10^6$ [25]
formate ion	$1.3×10^8$ [24]	$1.3×10^8$ [32]	–	$8.0×10^4$ [32]
formic acid	$1.6×10^7$ [24]	$3.2×10^7$ [32]	–	$<1×10^4$ [25]
acetic acid				
Acrylic compound	$5.7×10^9$ [24]	–	–	$1.9×10^7$ [25]
acrylate ion	$4.0×10^9$ [24]	–	–	$2.2×10^6$ [25]
acrylonitrile				
Benzene derivative	$7.8×10^9$ [24]	$6–12×10^9$ [28]	–	$<1×10^5$ [28]
benzene	$3.9×10^9$ [24]	0 [29]	–	0** [16]
nitrobenzene	$6.6–18×10^9$ [24]	–	–	$2.5–5×10^8$ [25]
phenol	–	–	$1.4×10^9$ [18]	$4.0×10^7$* [25]
4-cyanophenoxide ion	$7.6×10^9$ [24]	–	$1.5×10^9$ [18]	–
4-nitrophenoxide ion	$5.9×10^9$ [24]	–	$<3×10^6$ [18]	$2×10^6$ [25]
benzoate ion	$5.0×10^9$ [24]	–	–	$3×10^6$ [25]
4-chlorobenzoate ion	$7.0×10^9$ [24]	–	$1.1×10^9$ [18]	–
2,4,5-trimethoxybenzoate ion	$7.0×10^9$ [24]	–	$2.1×10^9$ [18]	–
1,4-dimethoxybenzene				

* This rate constant is of 4-cyanophenol.
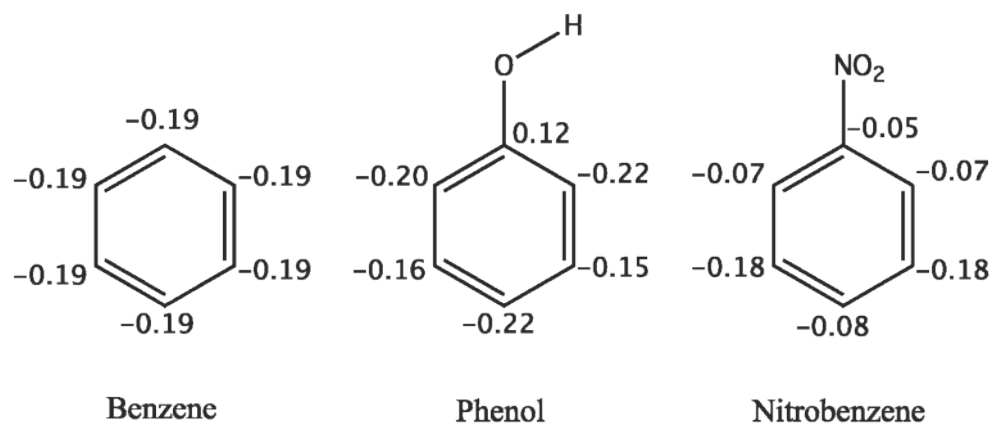** This is a hypothesis in the model by Fang *et al*.

Fig. 4 Löwdin charge of carbons in benzene derivatives calculated with GAMESS (18Aug2016R1). The calculation conditions were basis set: 6–31+G (d,p), self-consistent field (SCF) type: spin restricted Hartree-Fock method (RHF), run type: optimize, and polarized continuum model (PCM): water.

that RCS show relatively high reactivity with olefins and benzene derivatives and electron-donating groups promote the attack of benzene derivatives [23].

HO$^\cdot$ is known as a non-selective electrophilic reagent. Minakata *et al.* classified the reaction mechanisms of oxidation by HO$^\cdot$ as follows: H-abstraction, HO$^\cdot$ addition to alkenes, HO$^\cdot$ addition to aromatic compounds, and HO$^\cdot$ interaction with sulfur- (S-), nitrogen- (N-), or phosphorus- (P-) containing compounds [34]. They also developed a group contribution method to predict aqueous phase HO$^\cdot$ reaction rate constants. In this method an augmentation effect of each group on the rate constant is expressed by a group contribution factor. As a result, stronger contributors to HO$^\cdot$ reaction, namely functional groups with group contribution factor above 1, are as follows: -CH$_3$, -CH$_2$, >CH-, and >C< for H-abstraction, none for HO$^\cdot$ addition to alkenes, -NH$_2$, -OH, -NH-, and -O- for HO$^\cdot$ addition to benzene derivatives, -OH and -NH$_2$ for pyridine derivatives, -alkane and -O- for furan derivatives, -N<, -NH, and -alkane for imidazole derivatives, -NH$_2$ and -S- for triazine derivatives, and -N-CO-, -S-, -SS-, -HS-, -NH$_2$, -NH-, -N< for S-, N-, and P-atom containing compounds.

On reaction mechanisms of Cl$^\cdot$ Buxton *et al.* discussed the reactivity of Cl$^\cdot$ with oxy-organic compounds like acids, alcohols, aldehydes, and ketones in aqueous solution and concluded that the main mechanism of oxidation by Cl$^\cdot$ is preferential attack at O-H groups in neutral molecules and electron transfer in anions [32]. Minakata *et al.* suggested that Cl-adduct formation as well as H-abstraction is a major mechanism of oxidation by Cl$^\cdot$ [30]. Ezell *et al.* reported the reactivity of Cl$^\cdot$ with alkenes in gas phase and two oxidation mechanisms were proposed; the addition of Cl atom to double bond and abstraction of an allylic hydrogen atom, whereas the latter is slower than that of the analogous alkyl hydrogen atoms in alkanes [35].

On Cl$_2^{\cdot-}$ Hasegawa and Neta discussed the reactivity of Cl$_2^{\cdot-}$ with various organic compounds [36]. The main mechanisms of oxidation by Cl$_2^{\cdot-}$ are the H-abstraction for aliphatic compounds, Cl atom addition for olefinic compounds, and Cl atom addition to aromatic rings and the direct oxidation by electron transfer for aromatic compounds.

Information on reaction mechanism of ClO$^\cdot$ is relatively limited compared with other RCS. Kong *et al.* reported that degradation of gemfibrozil by ClO$^\cdot$ is initiated by hydroxylation and chlorine substitution on the benzene ring [37]. Alfassi *et al.* discussed the kinetics of ClO$^\cdot$ and suggested that ClO$^\cdot$ abstracts an electron from an organic compound and produces an organic radical like equation (10), but H-

abstraction or addition reaction is difficult to occur [18].

$$\text{Phenoxide ion } C_6H_5O^- + ClO^\cdot \rightarrow C_6H_5O^\cdot + ClO^- \quad (10)$$

Since ClO$^\cdot$ is produced from ClO$^-$ or HOCl through reactions with HO$^\cdot$, Cl$^\cdot$, or Cl$_2^{\cdot-}$, namely R$_1$, R$_2$, or R$_3$ in **Fig. 3** and **Table 1**, ClO$^\cdot$ acts as a mediator.

Recently, it was found that reaction rate constants of HO$^\cdot$ and chlorine-derived radicals are linearly correlated with theoretically calculated free energies of activation [30,38]. Such a computational chemistry approach will be useful for a deeper understanding of reactivity of reactive radical species in UV/chlorine AOPs. An example of the application of this approach to an UV/chlorine AOP is reported using acetone as a model pollutant [39].

Contribution of each radical species

As is described before, HO$^\cdot$ and RCS are main contributors to chemical oxidation by UV/chlorine AOPs. The contribution of each reactive species depends on not only its reactivity with chemical compounds but also its concentration in a reactor. The contribution of reactive species can be determined by a chemical probe method under a steady-state assumption. For instance, in order to evaluate the contribution of HO$^\cdot$ and RCS to degradation of pollutant, it is enough to add two chemical probes into the UV/chlorine reactor where following equations are established.

$$\frac{dC_{pollut}}{dt} = -k'_{pollut}\,C_{pollut} = -\left(k_{HO^\cdot - pollut}C_{HO^\cdot} + k_{RCS - pollut}C_{RCS}\right)C_{pollut} \tag{11}$$

$$\frac{dC_{P1}}{dt} = -k'_{P1}\,C_{P1} = -\left(k_{HO^\cdot - P1}C_{HO^\cdot} + k_{RCS - P1}C_{RCS}\right)C_{P1} \tag{12}$$

$$\frac{dC_{P2}}{dt} = -k'_{P2}\,C_{P2} = -\left(k_{HO^\cdot - P2}C_{HO^\cdot} + k_{RCS - P2}C_{RCS}\right)C_{P2} \tag{13}$$

where

k': pseudo first-order reaction rate constant observed [1/s],

k: second-order reaction rate constant [L/(mol·s)],

C: concentration [mol/L],

Subscripts of *pollut*, *HO$^\cdot$*, *RCS*, *P*1, *P*2 depict pollutant, HO$^\cdot$, RCS, chemical probe 1, and chemical probe 2, respectively.

The steady-state concentrations of HO$^\cdot$ ($C_{HO^\cdot}$) and RCS

(C_{RCS}) are obtained by solving equations (12) and (13) under the assumption of steady state. Then, the contribution of HO˙ $(P_{HO˙})$ and RCS (P_{RCS}) to the degradation of pollutant is determined by follows:

$$P_{HO˙} = \frac{k_{HO˙-pollut}}{k'_{pollut}} C_{HO˙} \tag{14}$$

$$P_{RCS} = \frac{k_{RCS-pollut}}{k'_{pollut}} C_{RCS} \tag{15}$$

Some researchers applied this method for UV/chlorine AOPs to estimate the contribution of reactive species [20,23,31,37,40]. However, the addition of chemical probes affects both the degradation rate of pollutant and the steady-state concentration of reactive species through competitive consumption of reactive species. Therefore, this method is not applicable to evaluating the contribution of reactive species in a practical application exactly.

The second approach to evaluate the contribution of reactive species is a chemical equilibrium method under the assumption of instantaneous equilibrium. In this method the concentration ratios among reactive species are obtained by the law of mass action. For instance, when the reaction scheme of UV/chlorine AOP is depicted in **Fig. 3**, chemical equilibrium among reactive radical species of HO˙, Cl˙, Cl_2˙⁻, and ClOH˙⁻ is formulated using equilibrium constants of K_1, K_2, and K_3 for chemical equilibrium of E_1, E_2, and E_3, respectively, as follows:

$$\frac{C_{Cl_2˙-}}{C_{Cl˙}C_{Cl^-}} = K_1 \tag{16}$$

$$\frac{C_{Cl˙}}{C_{ClOH˙-}C_{H^+}} = K_2 \tag{17}$$

$$\frac{C_{ClOH˙-}}{C_{HO˙}C_{Cl^-}} = K_3 \tag{18}$$

The radical concentration ratios are determined by solving these equations as follows:

$$\frac{C_{Cl_2˙-}}{C_{Cl˙}} = K_1 C_{Cl^-} \tag{19}$$

$$\frac{C_{ClOH˙-}}{C_{Cl˙}} = \frac{1}{K_2 C_{H^+}} \tag{20}$$

$$\frac{C_{HO˙}}{C_{Cl˙}} = \frac{1}{K_2 K_3 C_{H^+} C_{Cl^-}} \tag{21}$$

Thus, the radical concentration ratios depend on Cl⁻ concentration and pH. **Figure 5** shows the dependency of abundance of each radical to total radical concentration on Cl⁻ concentration and pH estimated by the abovementioned chemical equilibrium method using equilibrium constants of K_1, K_2, and K_3 shown in **Table 1**. **Figure 5** clearly shows Cl˙ and Cl_2˙⁻ are favorable to acidic condition, whereas basic condition is preferable for ClOH˙⁻ and HO˙. Although HO˙ and Cl˙ are primary radicals in UV/chlorine AOPs, the abundance of Cl˙ is relatively low; less than 0.01% at neutral pH. Domestic wastewater usually contains 200–500 mg/L of Cl⁻ that is equivalent to 5.6–14 mM [41]. Accordingly, the abundance of HO˙, Cl˙, Cl_2˙⁻, and ClOH˙⁻ in domestic wastewater at pH 7 is calculated to be in the range of 89–56, 0.010–0.016, 11–43, and 0.35–0.55% of total radicals, respectively. Thus, HO˙ and Cl_2˙⁻ are thought to be abundant in UV/chlorine AOPs in a typical wastewater. When pollutants are assumed to react with HO˙, Cl˙, Cl_2˙⁻, and ClOH˙⁻, the contribution of HO˙ to the pollutant degradation, $P_{HO˙}$, is determined using the radical concentration ratios as follows:

$$P_{HO˙} = \frac{k_{HO˙-pollut}C_{HO˙}}{k_{HO˙-pollut}C_{HO˙} + k_{Cl˙-pollut}C_{Cl˙} + k_{Cl_2˙--pollut}C_{Cl_2˙-} + k_{ClOH˙--pollut}C_{ClOH˙-}}$$

$$= \frac{k_{HO˙-pollut}\dfrac{C_{HO˙}}{C_{Cl˙}}}{k_{HO˙-pollut}\dfrac{C_{HO˙}}{C_{Cl˙}} + k_{Cl˙-pollut} + k_{Cl_2˙--pollut}\dfrac{C_{Cl_2˙-}}{C_{Cl˙}} + k_{ClOH˙--pollut}\dfrac{C_{ClOH˙-}}{C_{Cl˙}}} \tag{22}$$

The contribution of other species can be also determined by the similar manner. Kishimoto *et al.* applied this method to 1,4-dioxane degradation by an UV/electro-chlorine process under high Cl⁻ concentration of 85.5 mM, and estimated that the contribution of HO˙, Cl˙, and Cl_2˙⁻ to 1,4-dioxane degradation at pH 7 was 89.2, 0.003, and 10.8%, respectively, whereas the abundance of each radical was 0.88% for HO˙, 0.02% for Cl˙, and 99.1% for Cl_2˙⁻, because of a big difference in reaction rate constants of 1,4-dioxane with HO˙ and Cl_2˙⁻ [19]. This method can apply to exploring a practical application without any chemical probe. However, available
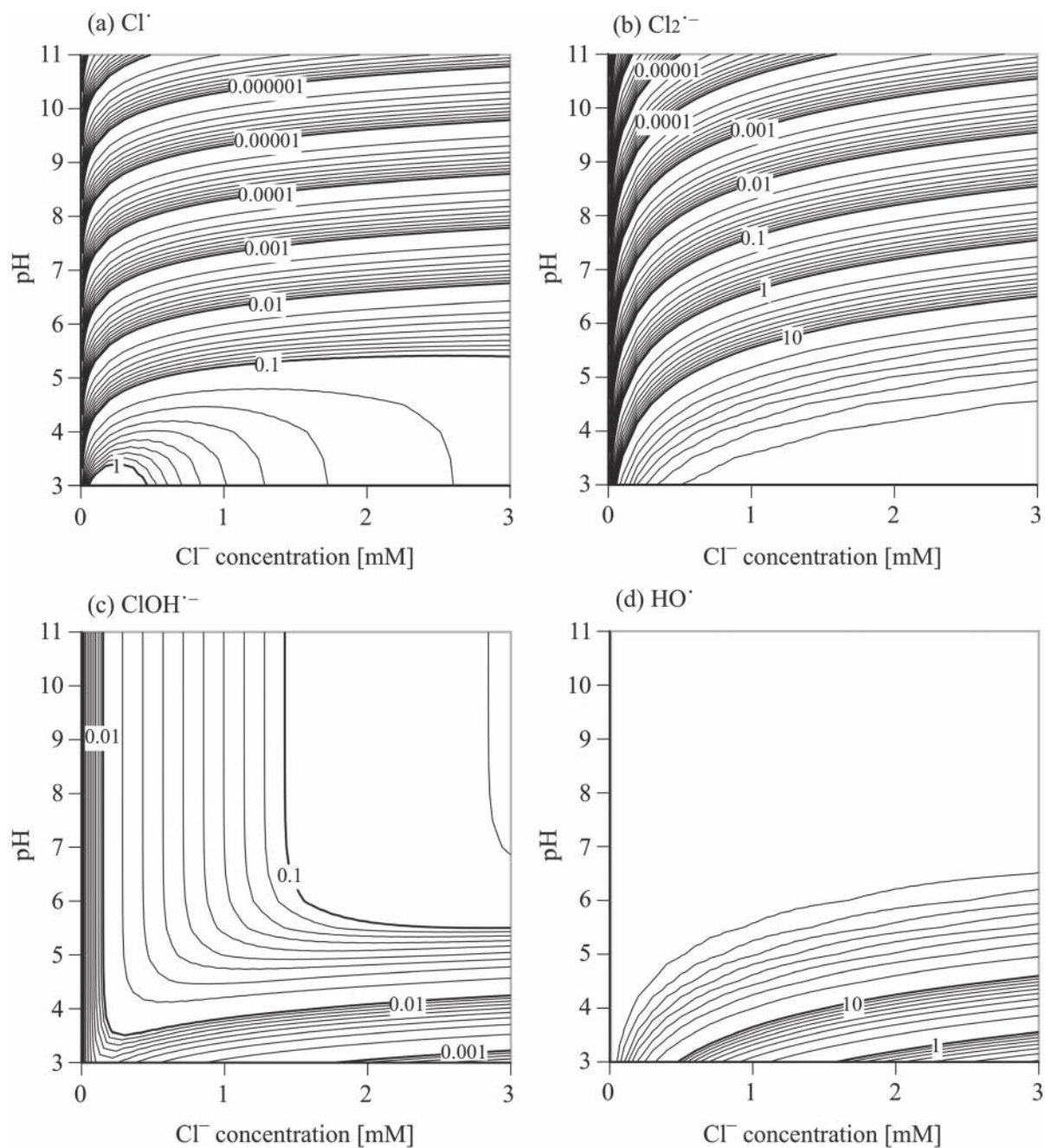
Fig. 5 Influences of Cl^- concentration and pH on percentage of $Cl^{\cdot}$, $Cl_2^{\cdot-}$, $ClOH^{\cdot-}$, and $HO^{\cdot}$ fractions to total radical concentration. Chemical equilibriums of E_1, E_2, and E_3 in **Fig. 3** and **Table 1** were used for calculation.

equilibrium constants reported in literatures contain various errors. Accordingly, the estimated results by this method also contain errors. For instance, the chemical equilibrium of E_4 instead of E_1 in **Fig. 3** and **Table 1** is used, the concentration ratio of $Cl_2^{\cdot-}$ to $Cl^{\cdot}$ is estimated to be 40% of that using E_1. As a result, the abundance of each radical is also changed as shown in **Fig. S1** in Supplementary Material, though the overall pattern does not change.

The third approach is a kinetics modeling method, where mass balance equations involving chemical kinetics of every species observed in a reactor are formulated. The mass balance equations are then solved by a computer-aided numerical calculation or steady state analysis. This method is the strictest solution for evaluating the contribution of reactive species. Moreover, it can determine concentrations of reactive radical species. However, it requires a detail reaction

scheme and a complete data set of reaction rate constants for a plenty of related reactions. Since available reaction rate constants contain various errors, the reliability of calculated results should be carefully discussed. Usually this method is available for evaluating concentrations of reactive radical species in order of magnitude level. Fang *et al.* used this method coupled with steady state analysis for analyzing the role of reactive species in an UV/chlorine system [16]. It should be noted that the aforementioned chemical equilibrium method is regarded as a derivative of the kinetics modeling method with steady state analysis.

BYPRODUCTS FORMATION

Chlorate and perchlorate

Chlorate ion (ClO_3^-) is known as one of unfavorable disinfection byproducts (DBPs), which is produced through decomposition of HOCl and ClO^- as follows [42]:

$$2HOCl + ClO^- \rightarrow 2Cl^- + ClO_3^- + 2H^+ \tag{23}$$

$$3ClO^- \rightarrow 2Cl^- + ClO_3^- \tag{24}$$

The equation (24) involves following two-step reactions.

$$2ClO^- \rightarrow ClO_2^- + Cl^- \text{ (slow)} \tag{25}$$

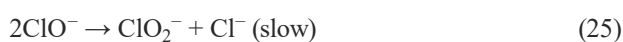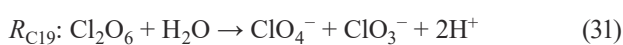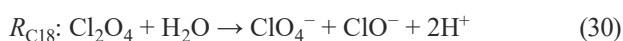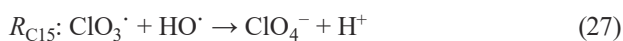$$ClO^- + ClO_2^- \rightarrow ClO_3^- + Cl^- \text{ (fast)} \tag{26}$$

In addition to the above pathways, ClO_3^- is produced through radical chain reactions. Kishimoto *et al.* summarized the chemical and photochemical reaction schemes related to oxychlorides [19]. They considered oxychlorides with the oxidation state from Cl (I) to Cl (VI), namely from ClO^- to $ClO_3^{\cdot}$. However, $ClO_3^{\cdot}$ further causes a reaction with $HO^{\cdot}$, $ClO^{\cdot}$, or $ClO_3^{\cdot}$ and finally produces perchlorate ion (ClO_4^-) as follows [43–45]:

$$R_{C15}: ClO_3^{\cdot} + HO^{\cdot} \rightarrow ClO_4^- + H^+ \tag{27}$$

$$R_{C16}: ClO_3^{\cdot} + ClO^{\cdot} \rightarrow Cl_2O_4 \tag{28}$$

$$R_{C17}: 2ClO_3^{\cdot} \rightarrow Cl_2O_6 \tag{29}$$

$$R_{C18}: Cl_2O_4 + H_2O \rightarrow ClO_4^- + ClO^- + 2H^+ \tag{30}$$

$$R_{C19}: Cl_2O_6 + H_2O \rightarrow ClO_4^- + ClO_3^- + 2H^+ \tag{31}$$

where R_{CXX} corresponds to that in **Fig. 6** and **Table 1**.

Since UV/chlorine system involves free chorine, $HO^{\cdot}$, and $ClO^{\cdot}$, ClO_3^- and ClO_4^- formation is also apprehended.

Fundamental and applied studies on UV/chlorine processes revealed that formation of ClO_4^- during UV/chlorine treatment was negligible [12,46,47]. However, ClO_3^- is one of major products of chlorine photolysis. Buxton and Subhani reported that the percentage of ClO_3^- conversion against free chlorine consumed was 17%-mole by photolysis of free chlorine at the wavelength of 254 nm and pH of 11.7 [12]. Feng *et al.* observed that the ClO_3^- conversion reached 14–24%-mole of free chlorine consumed by photolysis at 254 nm under pH 8.5, which were calculated from concentration data shown in their graph [46]. Rott *et al.* observed that 1.04 and 1.11 mg/L of ClO_3^- formation by an UV/chlorine AOP of effluent of a municipal wastewater treatment plant with free chlorine dose of 5 and 6 mg/L, respectively, which is equal to the ClO_3^- conversion ratio of 16–18%-mole [48]. Wang *et al.* reported that 2–14% of free chlorine consumed was converted to ClO_3^- in full and pilot scale water purification plants using medium pressure mercury vapor lamp at pH 6.5–8.5 [47]. They also reported that chlorite ion (ClO_2^-) derived from commercial sodium hypochlorite solution was decreased to less than 1% of initial concentration during UV/chlorine treatment at chlorine dose of 10 mg/L. Commercial chlorine solution contains ClO_2^-, ClO_3^-, and ClO_4^- at 0.2, 1–15, and 0.001–0.01%-weight of free chlorine concentration, respectively [47]. Therefore, we should pay attention to the ClO_3^- formation during UV/chlorine treatment.

Chlorinated organic compounds

Chlorinated organic compounds like halomethanes (HMs), haloacetic acids (HAAs), haloacetonitriles (HANs), haloketones (HKs), halonitoromethanes (HNMs), haloacetamides (HAAms), and chloral hydrate (CH) are well known DBPs by chlorination [49,50] and their formation in UV/chlorine AOPs is thereby apprehended. In fact some researchers reported that UV/chlorine AOPs produced trichloromethane (TCM) and chloroform (CF) in HMs, dichloroacetic acid (DCAA) and trichloroacetic acid (TCAA) in HAAs, dichloroacetonitrile (DCAN) and trichloroacetonitrile (TCAN) in HANs, dichloropropanone (DCP) and trichloropropanone (TCP) in HKs, chloronitoromethane (CNM), dichloronitoromethane (DCNM), and trichloronitromethane (TCNM) in HNMs, dichloroacetamide (DCAAm) and trichloroacetamide (TCAAm) in HAAms, and CH [20–22,37,47,51–55]. Some comparative studies of UV/chlorine process with chlorination have been reported. Pisarenko *et al.* observed the enhanced formation of chloroacetic acids by UV/chlorine treatment of Colorado River water, though the observed concentration of total HAAs was far below the US EPA regulated maximum

(A) Chemical reaction pathways
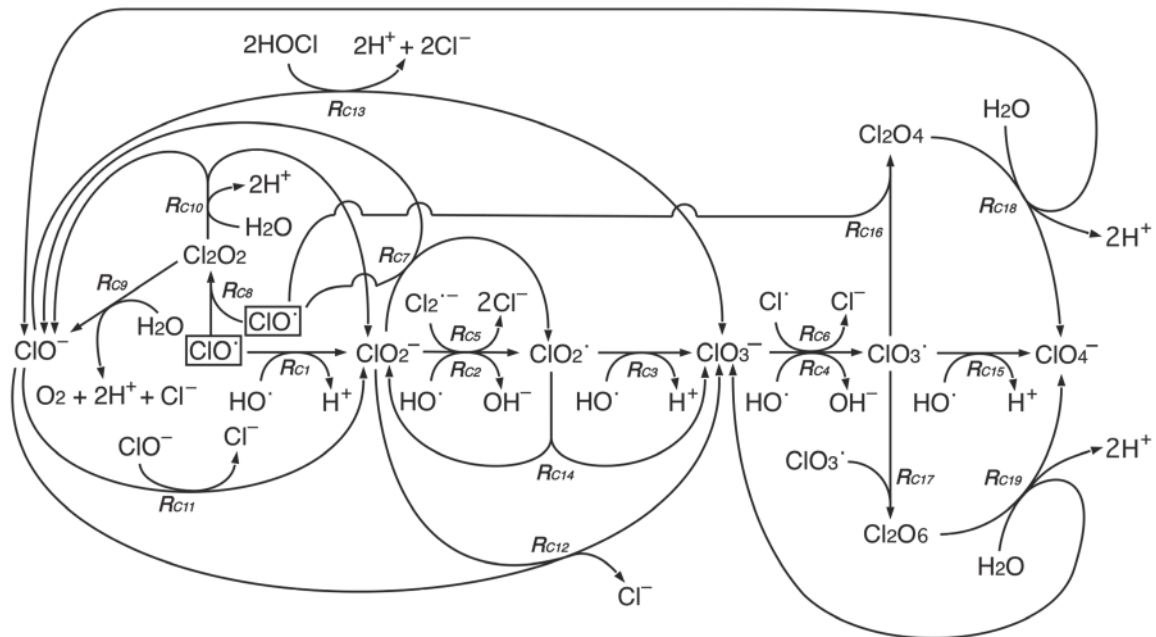
(B) Photochemical reaction pathways
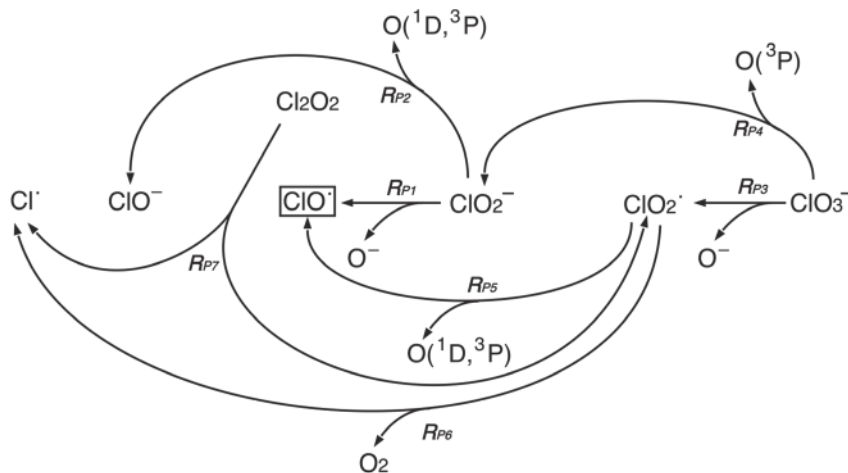
Fig. 6 Chemical and photochemical reaction schemes related to oxychlorides. The original figure in reference [19] is updated. An initiator of ClO$^\cdot$ is produced through reactions R_1, R_2, and R_3 in **Fig. 3**.

contaminant level [56]. Wang *et al.* reported that an UV/chlorine treatment of Lake Simcoe water enhanced the formation of HAAs and HANs at a weak acidic condition of pH 6.5, though the enhancement effect was not observed during the treatment of St. Lawrence River water at pH 8.5 [47]. In synthetic water treatment, TCM and DCAA formation is constrained by UV/chorine treatment of carbamazepine, but TCAA, DCAN, and TCNM formation is enhanced [51]. An UV/chlorine AOP of phenacetin decreased total DBPs formation due to the reduction of TCM formation despite the

enhanced formation of CH [54]. At post-chlorination stage, Lu *et al.* reported that post-chlorination with a chlorine dose of 1.0 mM following UV/chlorine pre-treatment of 0.05 mM clofibric acid solution with a chlorine dose of 1.0 mM did not produce DCAN, TCAN, HNMs, chloromethane and dichloromethane, but increased TCM formation [57].

The formation mechanisms of chlorinated organic compounds are basically thought to be the same as those by chlorination, where electrophilic substitution reaction is the primary attack [58]. The difference in DBPs fraction between

UV/chlorine AOPs and chlorination will be attributed to UV photolysis and radical reactions. For instance, cyanogen chloride formation from amino acids by UV/chlorine treatment is promoted by UV exposure of chlorinated imidazole and guanidine compounds that are byproducts of chlorination of amino acids [59]. TCNM formation from methylamines is inferred to involve a combination of radical oxidation and photo-enhanced chlorination reactions [60].

N-Nitrosodimethylamine (NDMA)

N-Nitrosodimethylamine (NDMA) is produced through chloramination, ozonation, chlorination, and UV photolysis of nitrogenous organic compounds like amines or organic compounds coexistent with chloramine or nitrite [61]. An investigation of NDMA formation potential of wastewater effluents revealed that hydrophilic, low-molecular weight nitrogenous organic compounds with less than 1 kDa contained most of the precursors of NDMA [62]. The most important mechanism of NDMA formation is thought to be a dichloramine pathway, where a nucleophilic attack of unprotonated secondary amines on dichloramine forms unsymmetrical dialkylhydrazine intermediate, which is then oxidized to the corresponding nitrosamine [61]. In ozonation it was reported that hydroxylamine and dinitrogen tetroxide (N_2O_4) are the critical species for NDMA formation [63]. The N_2O_4 is produced through the combination of two nitrogen dioxides (NO_2·) that are produced by an electron transfer from nitrite ion to HO·. In UV/chlorine AOPs free chlorine is added to polluted water as a source of primary radicals of HO· and Cl·. If the polluted water contains ammonium ions, the added free chlorines react with ammonium ions and form chloramines. Therefore, NDMA formation via the dichloramine pathway is expected during UV/chlorine AOPs of ammonium ion- or chloramines-containing water. In addition, the N_2O_4 pathway will be also valid in UV/chlorine AOPs because of their HO· generation capability. Soltermann *et al.* observed NDMA formation by UV-C irradiation to pool water, which was enhanced by the addition of chloramine and chlorinated dimethylamine [64]. The enhanced formation of NDMA was hypothesized to occur via the reaction of nitric oxide or peroxynitrite with secondary aminyl radical, which are produced by the photolysis of monochloramine and chlorinated secondary amine. However, they also reported that the increase in UV dose decreased the NDMA formation. Sichel *et al.* reported that NDMA was not detected in UV/chlorine treatment of synthetic wastewater similar to wastewater treatment plants (WWTP) effluents [65]. It is known that NDMA is directly photolyzed by UV light and produces dimethylamine and nitrite ion [66]. Accordingly, NDMA formation will not be a major byproduct of UV/chlorine AOPs.

INACTIVATION AND TOXICITY

Inactivation of microbes

Both of UV irradiation and chlorination are popular disinfection processes. Therefore, UV/chlorine AOPs are expected to be effective in disinfection. Rattanakul *et al.* discussed combination effects of UV and chlorine on inactivation of viruses [67]. As a result, the simultaneous application of UV irradiation and chlorination showed 2.3 times higher inactivation rate than the sum of inactivation rates by single application of UV irradiation and chlorination under the same UV fluence and chlorine dose, probably due to effect of radicals produced in UV/chlorine system. Li *et al.* reported the *Bacillus subtilis* spore inactivation by UV/chlorine AOPs with UV light-emitted diodes (UV-LED) [68]. The chlorine dose of 4.0 mg-Cl_2/L under the UV fluence of 125 mJ/cm^2 at pH 7 resulted in an additional 1.8-log and 1.5-log inactivation of *B. subtilis* spore by using 265 and 280 nm UV-LED, respectively. It was experimentally confirmed that the enhancement effects were caused by HO· produced in the UV/chlorine system. Zhou *et al.* observed >2 log inactivation of *Cryptosporidium parvum* oocysts by solar photolysis of free chlorine at 8 mg-Cl_2/L (CT value of 200 mg-Cl_2·min/L), whereas single applications of chlorination (CT value ≤832 mg-Cl_2·min/L) and solar irradiation achieved 0 and <0.5 log oocyst inactivation, respectively [69]. Thus, UV/chlorine processes have a synergic effect on disinfection due to a contribution of reactive radical species. Inactivation of *Microcystis aeruginosa* by an UV/chlorine process was investigated by Sun *et al.* [70]. As a result, the UV/chlorine process successfully enhanced the inactivation of *M. aeuginosa* especially at the chlorine dose ≥1.0 mg-Cl_2/L and was also effective in removing microcystin-LR released from *M. aeruginosa*. Furthermore, the UV/chlorine process improved the coagulation efficiency through improving zeta-potential of *M. aeruginosa* cells from −28.3 to −2.1 mV.

Crowe *et al.* discussed the antimicrobial efficacy of UV/chlorine treatment against bacterial flora on lowbush blueberries, where UV light was irradiated to lowbush blueberries just after spraying 100 mg-Cl_2/L of chlorinated water [71]. As a result, UV/chlorine treatment showed no synergistic effect on antimicrobial activity due to self-shadowing of lowbush blueberries against UV radiation. Thus, UV irradiation techniques are not effective in processing of particles.

Table 3 Toxicity change by applying UV/chlorine AOPs.

Test	Target	Process	Toxicity change	Ref.
luminescence inhibition (*Vibrio fischeri*)	phenol	UV/electro-chlorine	96% reduction by 2 h treatment	[72]
	oil sands process-affected water	Solar UV/chlorine	49–66% reduction by 7 h treatment	[73]
	trimethoprim	UV/chlorine	increase in inhibition (8 → 31%) by 7 min treatment, but lower than chlorination alone (52%)	[21]
	gemifibrozil	UV/chlorine	increase in inhibition (5 → 15%) by 13 min treatment, but lower than UV alone (31%)	[37]
	imidacloprid (IMD) thiacloprid (THIA)	UV/chlorine	58 and 47% reduction by 1 h treatment for IMD and THIA, respectively	[74]
	naproxen	UV/chlorine	increase in inhibition (46 → 57%) by 12 min treatment	[40]
luminescence inhibition (*Photobacterium phosphoreum*)	benzalkonium chloride	UV/chlorine	91% reduction by 2 h treatment lower than chlorination alone	[53]
luminescence inhibition (Q67)	phenacetin	UV/chlorine	increase in inhibition (9 → 23%) by 20 min treatment, but lower than chlorination alone (45%)	[54]
respiration inhibition (*Escherichia colli*)	5,5-diphenylhydantoin	UV/chlorine	decrease to non-toxic level by 10 min treatment lower than chlorination alone	[141]
cytotoxicity (human hepatoma cells (Hep3B))	microcystin-LR	UV/chlorine	7–37% increase in viability against UV or chlorination alone	[142]
Protein phosphatase inhibition assay	microcystin-LR	UV/chlorine	75.0% decrease for 10 min treatment	[94]
whole effluent toxicity (*Ceriodaphnia dubia*)	trichloroethylene in groundwater	UV/chlorine	almost no toxicity	[143]
estrogenic activity (E-screen assay)	WWTP effluent	MP-UV/chlorine	>97% removal at chlorine dose >5 mg/L	[48]

Toxicity

Table 3 summarizes applied results of several toxicity tests to UV/chlorine AOPs. Among various toxicity tests the luminescence inhibition test with *Vibrio fischeri* is most popular in UV/chlorine AOPs. The *V. fischeri* toxicity was decreased by UV/chlorine treatment in three researches [72–74]. However, an increase in toxicity was reported in the rest of three [21,37,40]. One of reasons of the discrepancy may be treatment time in UV/chlorine AOPs. In researches with reduction in *V. fischeri* toxicity, the treatment time was not shorter than 1 h [72–74], whereas the treatment time was set at 13 min or shorter in the research with the increase in the toxicity [21,37,40]. In UV/chlorine AOPs chlorinated organic byproducts are temporally produced. Accordingly, the toxicity will increase with the formation of toxic byproducts.

However, part of them are decomposed by a prolonged operation of UV/chlorine process [21,53,60], which will result in a decrease in toxicity. In fact, a temporal increase and following decrease in *V. fischeri* toxicity was observed in all researches where a negative effect of UV/chlorine treatment on the toxicity removal was reported [21,37,40].

Among other toxicity tests a negative effect of UV/chlorine treatment was only reported in the luminescence inhibition test using a luminescent bacterium Q67 [54]. In this research the inhibition rate peaked at 10 min treatment and then decreased. Thus, the situation was similar to the case of aforementioned *V. fischeri* toxicity.

In conclusion, toxicity of wastewater may be temporally increased by UV/chlorine treatment with an insufficient treatment time. However, a prolonged treatment will

improve the toxicity of treated water. Thus, optimization of the operational condition is important for toxicity control by UV/chlorine AOPs.

INFLUENTIAL FACTORS

Effect of pH

Many researchers have observed that acidic pH is better for UV/chlorine AOPs on removing organic pollutants such as amitriptyline hydrochloride [75], benzalkonium chloride [53], caffeine [31], chloramphenicol [22], diethyltoluamide [31], 1,4-dioxane [5], iodoform [76], methyl salicylate [75], metronidazole [31], nalidixic acid [31], naproxen [40], neonicotinoid insecticides [74], nitrobenzene [77], 2-phenoxyethanol [75], ronidazole [78], and taste and odor compounds [79]. Three mechanisms, namely a change in quantum yield of chlorine photolysis, equilibrium shifts of radical species, and radical scavenger effects of HOCl and ClO$^-$, are mainly responsible for the pH dependence of the performance of UV/chlorine AOPs.

Fang *et al.* reported that the quantum yields of HOCl and ClO$^-$ photolysis at 254 nm were 1.45 and 0.97, respectively [16]. Since pKa of HOCl is 7.44 [80], the quantum yield increases with decreasing pH and thereby HO$^.$ and Cl$^.$ formation by chlorine photolysis is enhanced in acidic pH.

The primary radicals in UV/chlorine AOPs are HO$^.$ and Cl$^.$ (Eq. (1) or (2)). Parts of these radicals are transformed into other radicals such as ClOH$^{.-}$ and Cl$_2^{.-}$ according to the law of mass action as illustrated in **Fig. 3**. Since the reaction scheme in **Fig. 3** involves OH$^-$ and H$^+$, the composition of radical species depends on pH. As is shown in **Fig. 5**, lower pH is suitable for RCS, whereas higher pH is preferable for HO$^.$. A shift in the composition of radical species changes the performance of UV/chlorine AOPs, because reactivity of organic pollutants depends on radical species. Surface and ground water usually contain Cl$^-$ at the concentration less than 2 mM. Assuming 1 mM of Cl$^-$ concentration, molar fractions of HO$^.$, Cl$^.$, ClOH$^{.-}$, and Cl$_2^{.-}$ are calculated to be 2.5, 0.51, 0.02, and 97.0% at pH 3, 71.7, 0.14, 0.05, and 28.1% at pH 5, and 99.5, 0.002, 0.07, and 0.39% at pH 7, respectively, by the chemical equilibrium method (Eq. (19–21)). Thus, it is expected that the relative contribution of HO$^.$ decreases at acidic pH, if pollutants are reactive with RCS. However, some researches show that contributions of both HO$^.$ and RCS increase with a decrease in pH [31,37,40,79]. This discrepancy can be explained by the radical scavenger effect of ClO$^-$ [5,16,40,77,79]. Since reaction rate constants of ClO$^-$ with HO$^.$, Cl$^.$, and Cl$_2^{.-}$ are higher than those of

HOCl (**Table 1**), the radical scavenging effect of free chlorine is stronger in basic pH than in acidic pH. Consequently, total radical concentration in acidic solution is higher than in basic solution. This fact indicates that excessive addition of free chlorine into an UV/chlorine reactor is disadvantageous to its advanced oxidation performance and thereby the optimization of free chlorine feed system is very important in the process design.

Reverse responses of the performance of UV/chlorine AOP to pH are sometimes observed. In the case of trimethoprim, ClO$^.$ plays the most important role in the degradation [21], whose formation is enhanced under basic condition through reactions R_1, R_2, and R_3 in **Table 1**. In the case of phenolic compounds of salbutamol, ractopamine, and bisphenol A, these chemicals are transformed into the corresponding phenoxides with increasing pH, which are richer in electrons and more reactive with RCS [23]. Paracetamol degradation is also enhanced at pH higher than 7.0 due to higher reactivity of ClO$^-$ with paracetamol than that of HOCl [81]. Thus, both dissociation processes and selectivity of reactive species reactions with a pollutant also influence the pH dependency of the performance of UV/chlorine AOPs.

Effect of chlorine dose

Free chlorine is a source of reactive radical species produced in UV/chlorine system. Accordingly, it is expected that an increase in chlorine dose enhances pollutant degradation through augmentation of radical production. In fact, some researchers reported that the degradation of carbamazepine, methylene blue, and trimethoprim were enhanced by an increase in chlorine dose [21,51,82,83]. However, free chlorine acts as a radical scavenger by reactions of R_1, R_2, and R_3 in **Table 1** and **Fig. 3**, which produce ClO$^.$. Accordingly, an excessive addition of free chlorine may inhibit pollutant degradation. Chan *et al.* observed that degradation rate of cyclohexanoic acid was enhanced with an increase in chlorine dose till 1.55 mM, but decreased under higher chlorine doses in the range of 1.55–7.5 mM [82]. The decrease in the degradation rate at the chlorine dose higher than 1.55 mM was inferred to attribute to the radical scavenging effect of ClO$^-$. Wu *et al.* reported that the concentration of ClO$^.$ increased linearly with an increase in chlorine dose, whereas the concentrations of HO$^.$ and carbonate anion radical (CO$_3^{.-}$) almost kept unchanged [31]. As a result, the degradation rate of ClO$^.$-reactive pollutants of caffeine and nalidixic acid were linearly enhanced with chlorine dose. The similar increase in ClO$^.$ contribution to trimethoprim degradation with chlorine dose was also observed [21]. Thus, ClO$^.$

produced through reactions of R_1, R_2, and R_3 will mainly contribute to the enhancement of pollutant degradation rate with an increase in chlorine dose. In evidence, degradation rates of ClO·-unreactive pollutants of metronidazole and diethyltoluamide were not enhanced by an increase in chlorine dose [31].

Effect of halide ion

An increase in Cl⁻ concentration promotes $Cl_2^{·-}$ formation from Cl· and HO· through chemical equilibriums of E_1, E_3, and E_4 in **Fig. 3** and **Table 1**. Therefore, performance of UV/chlorine AOPs may be influenced by Cl⁻ concentration. Lu *et al.* observed that clofibric acid degradation was partially inhibited by addition of Cl⁻ at not less than 25 mg/L, probably due to the formation of less reactive $Cl_2^{·-}$ [57]. The similar inhibition effect of Cl⁻ through the shift of HO· to $Cl_2^{·-}$ was reported by Li *et al.* in 1,4-dioxane degradation by an UV/chloramine process [84]. On the contrary, Yin *et al.* reported that thiacloprid degradation was enhanced by addition of 0.2 M Cl⁻, whereas imidacloprid degradation was slightly inhibited [74]. They inferred that the difference in reactivity of thiacloprid and imidacloprid with $Cl_2^{·-}$ brought the experimental results. In other researches on degradation of atrazine [85], C.I. Reactive Red 2 [86], and trimethoprim [21] by UV/chlorine AOPs, no positive and negative effect of Cl⁻ was observed. Thus, Cl⁻ effect is thought to depend on the reactivity of $Cl_2^{·-}$ with pollutants.

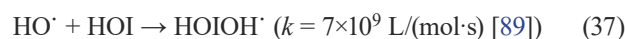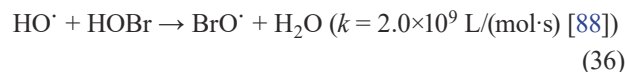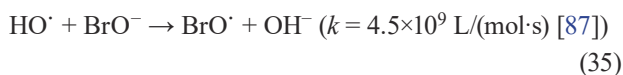When halide ions like bromide (Br⁻) and iodide (I⁻) are contaminated in water, they react with free chlorine as follows:

$$HOCl + X^- \rightarrow XCl + OH^- \tag{32}$$

$$HOCl + H^+ + X^- \rightarrow XCl + H_2O \tag{33}$$

$$XCl + 2OH^- \rightarrow XO^- + Cl^- + H_2O \tag{34}$$
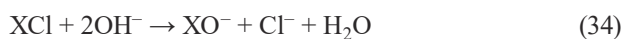
where

X: Br or I.

Reaction rate constants of Br⁻ and I⁻ are reported to be $1.55–6.84\times10^3$ and 1.4×10^8 L/(mol·s) for reaction (32) and 1.32×10^6 and 3.5×10^{11} L²/(mol²·s) for reaction (33), respectively [58]. Thus, heavier halide ion consumes free chlorine and produces hypohalite more rapidly. Hypohalites produced further scavenge HO· as follows:

$$HO· + BrO^- \rightarrow BrO· + OH^- \quad (k = 4.5\times10^9 \text{ L/(mol·s) [87]}) \tag{35}$$

$$HO· + HOBr \rightarrow BrO· + H_2O \quad (k = 2.0\times10^9 \text{ L/(mol·s) [88]}) \tag{36}$$

$$HO· + HOI \rightarrow HOIOH· \quad (k = 7\times10^9 \text{ L/(mol·s) [89]}) \tag{37}$$

Halide ions also react with HO· as follows:

$$HO· + X^- \rightarrow XOH^{·-} \tag{38}$$

Reaction rate constants of reaction (38) are 1.06×10^{10} and 1.1×10^{10} L/(mol·s) for Br⁻ and I⁻, respectively [24,90]. Although reaction rate constants of Cl· and halide ions are not reported, following Br⁻ and I⁻ oxidation by Cl· is expected, because standard electrode potentials of Br· and I· are lower than Cl·; 1.75–2.20 V vs. NHE for Br· and 1.27–1.42 V vs. NHE for I· [15].

$$Cl· + X^- \rightarrow Cl^- + X· \tag{39}$$

Consequently, halide ions and hypohalites act as scavengers of free chlorine and radicals, and thereby may deteriorate the performance of UV/chlorine AOPs. In fact, inhibitions of thiacloprid and iohexol degradation by Br⁻ were observed [74,91]. Zhao *et al.* reported that Br⁻ addition to an UV/chlorine reactor significantly lowered the steady state HO· concentration at pH 6.5, though the lowering effect of Br⁻ on HO· concentration was insignificant at pH 8.5 [92]. Although they did not show the reason of the pH dependency of experimental results, free chlorine consumption by BrCl formation through reactions (32) and (33) will be possible. Because the reaction rate constant of ClO⁻ with Br⁻ is reported to be 9×10^{-4} L/(mol·s) that is much smaller than the rate constant of reaction (32) for Br⁻ [58]. Thus, halide ion contamination should be heeded in UV/chlorine AOPs, especially under acidic condition. It should be noted that Br⁻ addition sometimes enhance degradation rates of pollutants that are reactive with reactive bromine species (RBS) like bromine (Br_2), bromine atom (Br·), dibromine radical ($Br_2^{·-}$), bromine oxide radical (BrO·), and chlorine bromide anion radical (ClBr$^{·-}$) [37,93,94].

BrO· is produced by reactions of free bromine and RCS in addition to reactions (35) and (36), and produces unfavorable bromate ion (BrO_3^-) through the similar mechanism of chlorate formation as shown in **Fig. 6**. Fang *et al.* reported that the formation of BrO_3^- is enhanced with the increases in UV fluence and pH [95]. The enhancement effect is stronger in UV-A irradiation than in UV-C irradiation due to the longer absorption peak wavelength of free bromine than that of free chlorine. Thus, Br⁻ contamination is problematic in BrO_3^- formation in addition to the inhibition by scavenging HO· and RCS.

Effect of alkalinity

In natural waters carbonate ion (CO_3^{2-}) and bicarbonate ion (HCO_3^-) are main contributors to alkalinity. They react with $HO^{\cdot}$, $Cl^{\cdot}$, and $Cl_2^{\cdot-}$ and produce $CO_3^{\cdot-}$, which may transform into carbonate radical ($HCO_3^{\cdot}$) according to pH.

$$CO_3^{2-} + HO^{\cdot} \rightarrow CO_3^{\cdot-} + OH^- \; (k = 3.9 \times 10^8 \text{ L/(mol·s) [24])}$$
$$(40)$$

$$HCO_3^- + HO^{\cdot} \rightarrow CO_3^{\cdot-} + H_2O \; (k = 8.5 \times 10^6 \text{ L/(mol·s) [24])}$$
$$(41)$$

$$CO_3^{2-} + Cl^{\cdot} \rightarrow CO_3^{\cdot-} + Cl^- \; (k = 5.0 \times 10^8 \text{ L/(mol·s) [96])}$$
$$(42)$$

$$HCO_3^- + Cl^{\cdot} \rightarrow CO_3^{\cdot-} + H^+ + Cl^- \; (k = 2.2 \times 10^8 \text{ L/(mol·s) [96])}$$
$$(43)$$

$$CO_3^{2-} + Cl_2^{\cdot-} \rightarrow CO_3^{\cdot-} + 2Cl^- \; (k = 1.6 \times 10^8 \text{ L/(mol·s) [97])}$$
$$(44)$$

$$HCO_3^- + Cl_2^{\cdot-} \rightarrow CO_3^{\cdot-} + H^+ + 2Cl^- \; (k = 8 \times 10^7 \text{ L/(mol·s) [97])}$$
$$(45)$$

$$CO_3^{\cdot-} + H^+ \leftrightarrow HCO_3^{\cdot} \; (pK_a = 7.9{-}9.6 \text{ [25])}$$
$$(46)$$
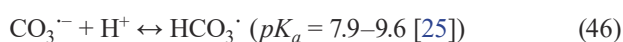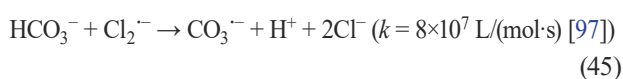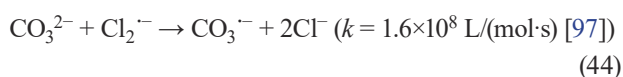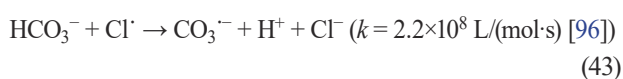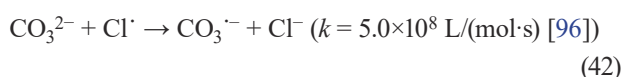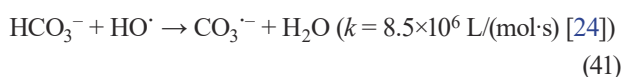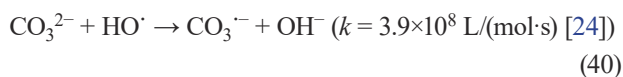
$CO_3^{\cdot-}$ produced consumes free chlorine as follows:

$$CO_3^{\cdot-} + ClO^- \rightarrow CO_3^{2-} + ClO^{\cdot} \; (k = 8.5 \times 10^6 \text{ L/(mol·s) [24])}$$
$$(47)$$
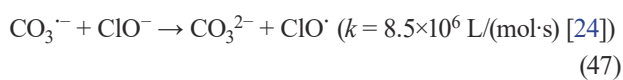
Thus, alkalinity may inhibit UV/chlorine AOPs through scavenging reactive radical species and free chlorine. Inhibition of UV/chlorine AOPs by alkalinity was reported in many papers on degradation of benzoic acid [16], caffeine [31], carbamazepine [83], diethyltoluamide [31], diuron [55], iodoform [76], metronidazole [31], nalidixic acid [31], and phenacetin [54]. But, alkalinity had no or negligible inhibition effect on degradation of atrazine [85], C.I. Reactive Red 2 [86], clofibric acid [57], imidazole [74], naproxen [40], thiacloprid [74], and trimethoprim [21]. Since the standard electrode potential of $CO_3^{\cdot-}$ was reported to be 1.59 V vs. NHE [17], it is expected to be a selective oxidant. Accordingly, the difference in alkalinity effect on degradation of pollutants depends on the reactivity of $CO_3^{\cdot-}$ with pollutants. Yin et al. reported that the inhibition effect of bicarbonate on imidazole and thiacloprid degradation was slight, because reactive $CO_3^{\cdot-}$ produced compensated for the loss of $HO^{\cdot}$, $Cl^{\cdot}$, and $Cl_2^{\cdot-}$ [74]. Pan et al. also pointed out that $CO_3^{\cdot-}$ produced contributed to the naproxen degradation to compensate for the loss of $HO^{\cdot}$ [40]. Guo et al. showed that steady-state concentrations of $HO^{\cdot}$, $Cl^{\cdot}$, and $Cl_2^{\cdot-}$ decreased in the presence of 1 mM bicarbonate, whereas $CO_3^{\cdot-}$ concentration increased and reached 3–6 orders of magnitude higher than those of $HO^{\cdot}$ and $Cl^{\cdot}$ [23]. These reports suggest the importance of $CO_3^{\cdot-}$ reactivity on understanding alkalinity effect.

Effect of natural organic matter (NOM)

Dissolved organic matter in aquatic systems originates from various sources. Some is transported from the surrounding landscape, is discharged by human activities, and is created in situ through microbial activity [98]. Organic matter supplied into the water body is affected by physicochemical and biochemical actions, and consequently its labile fraction is decreased. The residual stable fraction is thought to be mainly composed of fluvic acids. Natural organic matter contains aromatic C=C, methoxyl ($-OCH_3$), carboxylic, alcoholic, phenolic, and ketonic functional groups, etc [99]. But aquatic NOM has smaller elemental contents in carbon and nitrogen and higher ones in oxygen and sulfur than soil humic acids, and its aromaticity is lower than that of soil humic acids [99]. Although NOM is relatively stable, it easily reacts with $HO^{\cdot}$ and RCS. Accordingly, it will inhibit the degradation of pollutants by scavenging $HO^{\cdot}$ and RCS. Furthermore, since aquatic NOM absorbs UV and visible lights at a wavelength less than 500 nm [100], it will also lower the degradation rate of pollutants by shielding free chlorine and pollutants from UV light. Inhibition of UV/chlorine AOPs by NOM addition was reported in many papers on degradation of atrazine [85], bezafibrate [37], caffeine [31], carbamazepine [51], diethyltoluamide [31], diuron [55], gemfibrozil [37], iodoform [76], metronidazole [31], nalidixic acid [31], phenacetin [54], and trimethoprim [21]. Kong et al. reported that the inhibition of clofibric acid degradation by 1 mg-C/L of NOM was not observed, whereas the degradation of bezafibrate and gemfibrozil were clearly inhibited [37]. In their research, NOM reduced the contribution of RCS to degradation of bezafibrate and gemfibrozil and did not change the contribution of $HO^{\cdot}$. Since clofibric acid was not decomposed by RCS, NOM did not affect its degradation. Wu et al. also reported that scavenging effect of NOM on RCS + $CO_3^{\cdot-}$ was higher than that on $HO^{\cdot}$ [31]. Guo et al. estimated the steady-state concentration of $HO^{\cdot}$ and RCS in the presence of 1 mg-C/L of NOM, which elucidated that NOM lowered $ClO^{\cdot}$ concentration more strongly than those of $HO^{\cdot}$, $Cl^{\cdot}$, and $Cl_2^{\cdot-}$ [23]. As a result, $ClO^{\cdot}$-reactive PPCPs like caffeine, carbamazepine, and gemfibrozil were strongly affected by the addition of NOM, but the degradation rates

of ClO⁻-unreactive PPCPs like ibuprofen, metronidazole, ronidazole, and ormidazole were not decreased [23]. These reports suggest that NOM influences the performance of UV/chlorine AOPs by scavenging RCS, especially ClO·.

Effect of UV light source

Low pressure mercury vapor UV lamps (LP-UV lamps) are widely used as an UV light source for UV/chlorine systems. In addition to LP-UV lamps, a variety of UV lamps are commercially available like medium pressure mercury vapor UV lamps (MP-UV lamps), excimer lamps (excimer-UV), and UV light-emitting diodes (UV-LED). Moreover, solar radiation is also discussed as a light source for UV/chlorine AOPs in a few researches.

LP-UV/chlorine process

The mercury pressure of LP-UV lamps is typically of the order of 1 Pa, where re-absorption of emitted light is weak [101]. Accordingly, the radiation spectrum of a low pressure mercury plasma is dominated by the two ground state resonance lines at 254 and 185 nm with the ratio of resonance line intensities of about 1:5 [101]. However, available radiations from a LP-UV lamp depend on its envelope material. The preferable envelope material is fused quartz, which transmits more than 85% and 50% or less of UV lights at 254 and 185 nm, respectively [102]. If 185 nm radiation is unnecessary, soft glass (sodium-barium-glass) is available, which transmits more than 80% of UV light at 254 nm, but cuts off 185 nm light [102]. Two papers have been published, in which effect of vacuum UV light (VUV light at 185 nm) emitted from LP-UV lamps on UV/chlorine AOPs was discussed [103,104]. Li *et al.* discussed methylene blue degradation using a VUV-emitted and VUV-free LP-UV/chlorine systems [103]. Although the photon fluence of the VUV light only accounted for 5.6% of that of the UV light at 254 nm in their system, the VUV-emitted LP-UV/chlorine process enhanced methylene blue degradation rate more than 2.5 times of that of the VUV-free LP-UV/chlorine process. Moreover, the degradation rate observed in the VUV-emitted LP-UV/chlorine process was >1.6 times higher than the sum of the degradation rates by direct VUV photolysis and the VUV-free LP-UV/chlorine reactions. They mentioned that the synergistic effect of VUV radiation on UV/chlorine system was mainly ascribed to the effective use of HO· for methylene blue removal through formation of longer-lived secondary radicals like ClO· produced by reaction R₁ in **Table 1**. The research group of Li *et al.* also discussed sulfamethazine degradation using the same system and observed similar

results, namely >1.6-times higher degradation rate by the VUV-emitted LP-UV/chlorine process than the sum of those by the controls [104].

MP-UV/chlorine process

The mercury pressure of MP-UV lamps is in the range of 100–600 kPa, which is much higher than that of LP-UV lamps, which leads to a continuous radiation spectrum mainly composed of broadened and partly self-absorbed resonance lines [102]. Since ClO⁻ has a larger molar extinction coefficient around 300 nm than that at 254 nm (**Fig. 2**), MP-UV lamps may efficiently photolyze free chlorine, especially at a basic pH. Wang *et al.* applied a MP-UV/chlorine process to trichloroethylene degradation [105]. As a result, the fluence-based decay rate of free chlorine was enhanced with the increase in pH and was much higher than that of H_2O_2. However, the MP-UV/chlorine process at pH 7.5 and 10 had smaller fluence-based decay rates of trichloroethylene than the MP-UV/H_2O_2 process, whereas the former was superior to the latter at pH 5. As is mentioned in "Effect of pH" section, ClO⁻ is a stronger radical scavenger than HOCl. Therefore, the enhancement of radical scavenger effect at a basic pH was thought to lead to the decrease in trichloroethylene degradation performance of the MP-UV/chlorine process. Kedir *et al.* compared a MP-UV/chlorine system with a LP-UV/chlorine one on the degradation of methyl tertiary butyl ether [106]. Although the UV fluence of the LP-UV lamp was only about one eighth of that of the MP-UV lamp, more than 99% removal of 1000 ppb methyl tertiary butyl ether was achieved with the both systems. However, the LP-UV/chlorine system was more than 13.6 times superior to the MP-UV/chlorine system on energy efficiency. The highest UV peak of MP-UV lamp was 365 nm that is not effectively absorbed by free chlorine as shown in **Fig. 2**. Therefore, the energy efficiency of the MP-UV/chlorine system would be much lower than that of the LP-UV/chlorine system. A comparison study on UV-C at 254 nm and UV-A at 365 nm for UV/chlorine AOPs also revealed that UV-A is less effective than UV-C [56]. Thus, the use of MP-UV lamps is not recommended in UV/chlorine AOPs.

Excimer-UV/chlorine process

Excimer lamps use an emission from excited dimer, namely excimer. Commercially available excimer lamps emit quasi-monochromatic radiation at 126 nm (Ar₂*), 146 nm (Kr₂*), 172 nm (Xe₂*), 222 nm (KrCl*), or 308 nm (XeCl*) [107]. Radiation efficiencies of excimer lamps are reported to be <18% [101]. There is no report on excimer-UV/chlorine

AOPs. However, since it was reported that VUV-emitted LP-UV/chlorine processes has a synergistic effect on pollutants removal compared with VUV-free LP-UV/chlorine process and VUV photolysis [103,104], excimer lamps using Ar_2^*, Kr_2^*, or Xe_2^* may enhance the performance of UV/chlorine AOPs. A XeCl* excimer lamp is another candidate of an UV light source for UV/chlorine AOPs at a basic pH, because emission spectrum of XeCl* excimer lamp accords with the absorption peak of ClO^- (**Fig. 2**) and unavailable longer UV light is not radiated.

UV-LED/chlorine process

UV-LED is a newcomer of UV light source for water treatment filed. The emission wavelength of UV-LED depends on semiconductor structure and composition. Nowadays, UV-LEDs with emission wavelength of 210–365 nm using AlGaN structures with different composition are commercially available at research grade and in limited quantities [108]. Kwon *et al.* compared a 275 nm UV-LED/chlorine process with a LP-UV/chlorine process and indicated that the 275 nm UV-LED/chlorine system had higher radical yields at pH 7 and 8 than the LP-UV/chlorine system due to the higher ε of ClO^- at 275 nm than that of HOCl (**Fig. 2**) [109]. Wang *et al.* discussed the use of UV-LEDs with emission wavelength of 285 and 310 nm for UV/chlorine AOPs [110]. The UV-LED/chlorine processes showed one-order higher carbamazepine degradation rates than UV-LED/H_2O_2 processes. UV-LED with 285 nm was slightly superior to that with 310 nm, probably due to higher ε at 285 nm compared with at 310 nm (**Fig. 2**). The electrical energy per order reduction of pollutant (EE/O) of UV-LED/chlorine AOPs was 1.5–1.6 kWh/(m^3·order), which was less effective than that of LP-UV/chlorine AOPs due to lower emission efficiencies of UV-LEDs (ca. 2%) than LP-UV lamps (30–40%) [110]. Thus, a further progress in UV-LED technologies will be required for practical application of UV-LED for UV/chlorine AOPs.

Solar/chlorine process

Solar radiation has a radiation spectrum mainly in the range of 300–2400 nm and UV radiations energy (<400 nm) accounts for 8% of total extraterrestrial radiation [111]. Although about a half of them is not available to photolyze ClO^-, ClO^--sensitive extraterrestrial solar radiation is about 50 W/m^2 outside the earth. Thus, the solar radiation seems to be applicable to chlorine photolysis. Solar/chlorine AOPs are discussed in a few papers. Chan *et al.* performed methylene blue and cyclohexanoic acid degradation with a solar/chlorine process at pH 10 and observed pseudo first-

order degradation constants of 5.15×10^{-3} s^{-1} for 0.039 mM methylene blue and 3.75×10^{-4} s^{-1} for 0.23 mM cyclohexanoic acid [82]. Shu *et al.* applied a solar/chlorine process for oil sands process-affected water remediation [73]. The solar/chlorine process in the chlorine dose of 200 or 300 mg/L was successfully removed 75–84% of initial naphthenic acids (21.6 mg/L) for 7 h. However, since only a few experimental runs were performed in these researches, a further research will be required for optimizing the process. In the effect of visible light on pollutants degradation Izadifard *et al.* discussed chlorination combined with blue light irradiation at 440 nm from blue-LEDs (B-LED/chlorine process) [112]. Although free chlorine does not absorb the blue light, Swannee River fluvic acid solution was decolorized by the B-LED/chlorine process, while chlorination in dark was less effective in decolorization and direct B-LED photolysis was not observed. They postulate that fluvic acid photochemically excited by blue light reacted with free chlorine. The similar mechanism may also contribute to pollutants degradation by solar/chlorine processes.

The formation of DBPs during a solar/chlorine process was discussed by Young *et al.* [113]. The solar/chlorine process was found to yield depletion of dissolved organic chromophores and fluorophores, preferential removal of phenolic groups, and degradation of larger humic substances to smaller molecular weight compounds. However, it produced higher levels of DBPs like trihalomethanes (THMs) and HAAs than dark chlorination due to co-exposure of dissolved organic matter (DOM) to free chlorine and reactive species generated by free chlorine photolysis. Consequently, they commented that application of solar/chlorine processes would require careful attention to potential impacts on DBP formation.

Comparison with other UV-based AOPs

There are various UV-based AOPs like UV-photolysis of hydrogen peroxide (UV/H_2O_2), ozone (UV/O_3), and persulfate (UV/$S_2O_8^{2-}$). The primary radicals produced by these AOPs are different one another. Hydrogen peroxide is photolyzed by UV <310 nm and produces two $HO^•$ (Eq. (48)) [114], whereas persulfate ion is photolyzed through a simple O–O bond scission and produces two sulfate radical ($SO_4^{•-}$) (Eq. (49)) [115].

$$H_2O_2 + h\nu \rightarrow 2HO^• \tag{48}$$

$$S_2O_8^{2-} + h\nu \rightarrow 2SO_4^{•-} \tag{49}$$

The radical production mechanism of UV/O_3 is more com-

plicated than UV/H_2O_2 and UV/$S_2O_8^{2-}$. The UV-photolysis of O_3 produces H_2O_2 at an initial step (Eq. (50)), and then HO˙ are produced through UV-photolysis of H_2O_2 (Eq. (48)) and/or chain reactions of H_2O_2 with ozone (Eq. (51–56)) [14].

$$O_3 + H_2O + hv \rightarrow H_2O_2 + O_2 \tag{50}$$

$$H_2O_2 \leftrightarrow HO_2^- + H^+ \tag{51}$$

$$O_3 + HO_2^- \rightarrow O_3^{˙-} + HO_2^˙ \tag{52}$$

$$HO_2^˙ \leftrightarrow O_2^{˙-} + H^+ \tag{53}$$

$$O_3 + O_2^{˙-} \rightarrow O_3^{˙-} + O_2 \tag{54}$$

$$O_3^{˙-} + H^+ \leftrightarrow HO_3^˙ \tag{55}$$

$$HO_3^˙ \rightarrow HO^˙ + O_2 \tag{56}$$
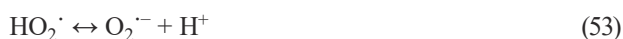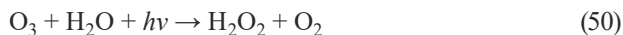
Consequently, overall reactions of radical production by UV/O_3 can be summarized as follows:

$$O_3 + H_2O + hv \rightarrow 2HO^˙ + O_2 \ (\text{H}_2\text{O}_2 \text{ photolysis pathway}) \tag{57}$$

$$3O_3 + H_2O + 2H^+ + hv \rightarrow 2HO^˙ + 4O_2 + 2H^+ \ (\text{chain reaction pathway}) \tag{58}$$

Thus, the differences in primary radical species and stoichiometric ratio of original oxidant to radical produced will bring a different impact on advanced oxidation performance.

Many comparison studies of UV/chlorine and UV/H_2O_2 have been reported. Part of them are summarized in **Table 4**. Although degradation performances depend on target pollutants, degradation rate constants of UV/chlorine are usually equivalent to or higher than those of UV/H_2O_2, especially at neutral or acidic pH. The decline in degradation performance in alkaline region is owing to the shift of free chlorine species from HOCl to ClO$^-$, which decreases the quantum yield of free chlorine and enhanced the scavenger effect on HO˙ and Cl˙ as described in the section "Effect of pH". Some researchers discussed the key radical species in UV/chlorine and UV/H_2O_2 and concluded that HO˙ is a main contributor in UV/H_2O_2, but $CO_3^{˙-}$ and RCS like ClO˙ play important roles in UV/chlorine [40,116,117]. In addition, contributions of RBS like Br˙ and $Br_2^{˙-}$ to PPCPs degradation in UV/chlorine AOPs are also pointed out, when Br$^-$ is contaminated [117]. Thus, reactivity of pollutant with secondary radicals like $CO_3^{˙-}$ and ClO˙ will influence the relative performance of UV/chlorine against other UV-based AOPs. Base on the reported information shown in **Table 4**, the electric energy and the chemical cost of UV/chlorine seem to be generally lower than those of UV/H_2O_2 required for achieving the same effluent water quality.

There is limited information on a comparison of UV/chlorine with UV/O_3. Hurwitz et $al.$ discussed phenol degradation by UV/H_2O_2, UV/O_3, and UV/chlorine with continuous anodic oxidation of Cl$^-$ (UV/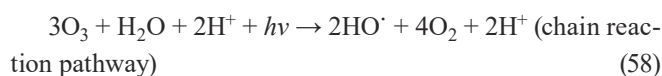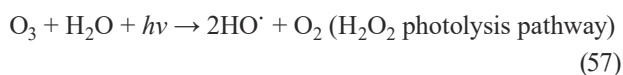electro-chlorine) [72]. As a result, UV/O_3 showed a higher mineralization rate (0.40 h^{-1}) than UV/electro-chlorine (0.38 h^{-1}) and UV/H_2O_2 (0.32 h^{-1}), whereas the electric energy per an order reduction of pollutant (EE/O) of UV/O_3 was the worst of the three; 189, 122, 104 kWh/(m^3·order) for UV/O_3, UV/H_2O_2, and UV/electro-chlorine, respectively. The higher mineralization rate by UV/O_3 is thought to be owing to direct oxidation of phenol by ozone, because phenol is easily oxidized by ozone with a second-order reaction rate constant of 1.3×10^3 L/(mol·s) [25]. The EE/O of UV/electro-chlorine is higher than that of UV/chlorine due to the electric power consumption by anodic oxidation of Cl$^-$. It should be noted that UV/electro-chlorine showed the lowest EE/O of the three regardless of disadvantage of the energy consumption for chlorine production.

Some papers dealt in the comparison of UV/chlorine with UV/$S_2O_8^{2-}$. The literature information is summarized in **Table 5**. Among five literatures in **Table 5** two papers demonstrate the lower degradation performance of UV/chlorine than that of UV/$S_2O_8^{2-}$ and the rest of three show the higher performance of UV/chlorine. Thus, UV/chlorine has advanced oxidation potential at least similar to UV/$S_2O_8^{2-}$, though the performance strongly depended on reactivity of target pollutant with reactive radical species. Varanasi et $al.$ pointed out that primary oxidation in UV/$S_2O_8^{2-}$ system is reactions of $SO_4^{˙-}$ with aromatic and olefinic structures and the reactivity of $SO_4^{˙-}$ with aliphatic acids and alcohols are lower than that of HO˙ and Cl˙ [118]. Furthermore, they also demonstrated that UV/$S_2O_8^{2-}$ system enhances the oxidation of CHNOS-containing compounds, but oxidizes CHNO-containing compounds less effectively than UV/chlorine system. In **Table 5** UV/$S_2O_8^{2-}$ processes showed lower degradation rates in aniline, sulfamethoxazole, amitriptyline, methyl salicylate, 2-phenoxyethanol, phenacetin, C_4-imidazolium, and C_4-pyridium than UV/chlorine processes. These 8 chemicals are composed of two CHO-, five CHNO-, and one CHNOS-containing compounds. This result approximately accords with the reactivity reported by Varanasi et $al.$ Thus, UV/chlorine system may be more favorable to degradation of CHNO-containing compounds than UV/$S_2O_8^{2-}$ system.

Table 4 Relative performance and efficiency of UV/chlorine AOP against UV/H_2O_2 AOP.

Target	Performance	Efficiency	Note	Ref.
benzoate, carbamazepine, 1,4-dioxane	Superior for carbamazepine Superior at pH 5.5, but inferior at pH ≥7.0 for benzoate and 1,4-dioxane	–	pH5.5–8.3	[124]
caffeine, carbamazepine, metoprolol, sulfamethoxazole	Superior for carbamazepine and metoprolol Equivalent for caffeine and sulfamethoxazole	–	pH 7 chlorine molar dose < H_2O_2 molar dose	[144]
naproxen	Superior at all pH tested	–	pH 6–9 key radical: HO˙ (UV/H_2O_2), ClO˙ and $CO_3^{˙-}$ (UV/chlorine)	[40]
nitrobenzene	Superior at pH 5 and 6 Inferior at pH 7	C/O <0.1 US$/($m^3$·order) at pH 5 (ca. half of C/O of UV/H_2O_2)		[77]
phenacetin	4.2 times higher degradation rate constant	EE/O [kWh/(m^3·order)]: 7.74 for UV/chlorine 32.90 for UV/H_2O_2	pH 7.2	[54]
phenol	Superior	EE/O [kWh/(m^3·order)]: 104 (85% of EE/O of UV/H_2O_2)	pH 8.3 UV/electro-chlorine	[72]
trichloroethylene in groundwater	Almost completely removed	Chemical cost reduction of 85%	pH 7.1–7.7	[143]
8 emerging contaminants	Superior for 5 chemicals Inferior for 3 chemicals	Energy reductions of 30–75%	pH 7	[65]
10 PPCPs in drinking water	Superior for all PPCPs	–	pH 7 chlorine molar dose < H_2O_2 molar dose	[131]
28 PPCPs in pure water, simulated drinking water, and real WWTP effluent	Superior for 16 PPCPs in pure water Superior for 27 PPCPs in simulated drinking water and real WWTP effluent	EE/O in real WWTP effluent [kWh/(m^3·order)]: 0.06–4.5 for UV/chlorine 0.2–8.1 for UV/H_2O_2	pH 7	[117]
6 trace organic contaminants	Superior for 3 chemicals Inferior for 3 chemicals	–	pH 5.8 key radical: HO˙ (UV/H_2O_2), $CO_3^{˙-}$ (UV/chlorine)	[116]
3 taste and odor chemicals in drinking water	Superior at pH 6.5 Superior or equivalent at pH >7.5	EE/O [kWh/(m^3·order)]: 0.16–0.87 for UV/chlorine 0.23–2.2 for UV/H_2O_2	pH 6.5–8.5	[129]
ionic liquid cations	5.3–8.0 times higher degradation rate constants	–	pH 7 chlorine molar dose < H_2O_2 molar dose	[145]

C/O: cost per an order reduction of pollutant
EE/O: electric energy per an order reduction of pollutant
PPCPs: pharmaceuticals and personal care products
WWTP: wastewater treatment plant

Miklos *et al.* summarized the EE/O of various AOPs; ozonation, O_3/H_2O_2, UV/O_3, UV/H_2O_2, UV/$S_2O_8^{2-}$, UV/chlorine, UV/catalyst, photo-Fenton, electro-oxidation, electron beam, plasma, microwave, and ultrasound processes [119]. UV/chlorine AOPs showed the lowest EE/O in average and fourth lower EE/O in median. Thus, UV/chlorine is thought to be an energy-efficient and promising AOP.

Table 5 Relative performance and efficiency of UV/chlorine AOP against UV/$S_2O_8^{2-}$ AOP.

Target	Performance	Efficiency	Note	Ref.
6 trace organic contaminants	Superior for 2 chemicals Inferior for 4 chemicals	–	pH 5.8 key radical: $CO_3^{\cdot-}$ (UV/chlorine), $SO_4^{\cdot-}$ and $HO^{\cdot}$ (UV/$S_2O_8^{2-}$)	[116]
amitriptyline, methyl salicylate, 2-phenoxyethanol in secondary effluent	1.1–2.3 times higher degradation rate constants	–	pH 7.0–8.3	[75]
clofibric acid	11% lower degradation rate constant	12% higher EE/O 9% lower total cost		[57]
phenacetin	8.4 times higher degradation rate constant	EE/O [kWh/(m³·order)]: 7.74 for UV/chlorine 64.67 for UV/$S_2O_8^{2-}$	pH 7.2	[54]
ionic liquid cations	1.1–2.3 times higher degradation rate constants	–	pH 7 chlorine molar dose < $S_2O_8^{2-}$ molar dose	[145]

EE/O: electric energy per an order reduction of pollutant

PROCESS VARIATIONS

UV/electro-chlorine process

Free chlorine is supplied by addition of chlorine chemicals like sodium hypochlorite in most of UV/chlorine processes. When the concentration of target pollutants is less than mg/L, the chemicals addition is feasible, because the chlorine dose is very low. However, when an UV/chlorine process is applied to industrial wastewater treatment, chemical oxygen demand (COD) is often in the range of several hundreds to several thousands mg/L. In such a case, chlorine supply by adding chlorine chemicals would not be feasible due to requirement of plenty of the chemicals. A countermeasure to this situation is on-site production of free chlorine by anodic oxidation of Cl^- (Eq. (59–60)). Chlorine production by electrolysis is widely utilized in chemical industries [120].

$$2Cl^- \rightarrow Cl_2 + 2e^- \tag{59}$$

$$Cl_2 + H_2O \rightarrow HOCl + H^+ + Cl^- \tag{60}$$

The introduction of continuous anodic oxidation of Cl^- into an UV/chlorine process (UV/electro-chlorine) was firstly reported by Hurwitz et al. [72]. Typical UV/electro-chlorine reactors are shown in **Fig. 7**. Hurwitz et al. combined an UV-photochemical reactor with an electrochemical flow cell with a ruthenium oxide-coated titanium (Ti/RuO_2) anode (**Fig. 7 (a)**) and compared the developed UV/electro-chlorine process with UV/H_2O_2, UV/O_3, and electro-oxidation using a boron-doped diamond anode (EL-BDD) on phenol degra-

dation. The mineralization rate of phenol by EL-BDD was much lower than other processes, though EE/O of EL-BDD was the lowest of the four. The UV/electro-chlorine process was the most energy-efficient of the rest of three UV-based processes. Furthermore, the UV/electro-chlorine process decreased *V. fischeri* toxicity more rapidly than the EL-BDD process and produced byproducts of chloroform, total trihalomethane, dichloroacetic acid, trichloroacetic acid, total haloacetic acid, and perchlorate much less than the EL-BDD process.

Florêncio et al. applied a single-chamber UV/electro-chlorine reactor with Ti/$Ru_{0.3}Ti_{0.7}O_2$ mesh anode to synthetic textile wastewater treatment (**Fig. 7 (b)**) [121]. The UV/chlorine process enhanced COD and total organic carbon (TOC) removal rate from 73 and 62% in electro-oxidation alone to 86 and 92%, respectively, and successfully reduced the accumulation of organochlorine compounds.

In the UV/electro-chlorine process, the solution pH is elevated with the accumulation of free chlorine, because Eq. (59) inhibits the anodic oxidation of water (Eq. (61)) and thereby anodic proton production decreases.

$$2H_2O \rightarrow O_2 + 4H^+ + 4e^- \tag{61}$$

As is previously described, UV/chlorine processes prefer acidic pH. Accordingly, an extreme increase in pH should be avoided. Kishimoto et al. introduced a reagent-free pH control system by switching on and off the electrochemical flow cell according to pH into an UV/electro-chlorine process for 1,4-dioxane degradation (**Fig. 7 (c)**) [19]. When the
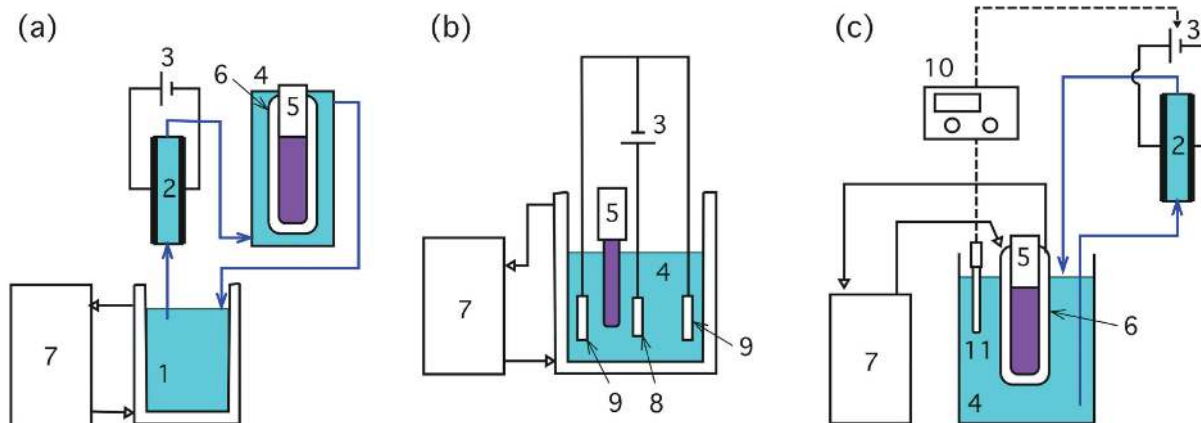
Fig. 7 Experimental setup of UV/electro-chlorine reactor
1: reservoir tank, 2: electrochemical flow cell, 3: DC power supply, 4: photochemical reactor, 5: UV lamp, 6: quartz sleeve, 7: thermostatic bath, 8: mesh anode, 9: counter cathode, 10: pH controller, and 11: pH sensor

active time of the cell against total time was in the range of 42–55%, pH and free chlorine concentration was maintained below 6.6 and 0.16 mM, respectively, whereas they reached the maximum of 7.7 and 0.51 mM without the pH control, respectively. The introduction of pH control successfully reduced 16–25% of energy consumption per 1,4-dioxane removal and 50–62% of chlorate and chlorite formation per 1,4-dioxane removal.

UV/NH$_2$Cl process

In some researches monochloramine (NH$_2$Cl) substituted for free chlorine in UV/chlorine processes (UV/NH$_2$Cl process), because chloramines contamination is expected in an application to swimming pool water and free chlorine is not preferable for a water reuse system with reverse osmosis membranes. The photolysis of NH$_2$Cl by UV light was reported to be as follows [122]:

$$NH_2Cl + h\nu \rightarrow NH_2^{\cdot} + Cl^{\cdot} \tag{62}$$

Amine radical (NH$_2^{\cdot}$) produced further reacts with NH$_2$Cl and molecular oxygen as shown in **Fig. 8** [64,84,122,123].

An application of UV/NH$_2$Cl process to 1,4-dioxane degradation revealed that Cl$_2^{\cdot-}$ and HO$^{\cdot}$ mainly contributed to 1,4-dioxane degradation, and the reactivity of NH$_2^{\cdot}$ was very limited [27]. Moreover, dissolved oxygen further decreased 1,4-dioxane degradation through the production of NO$^{\cdot}$ that negligibly impacted 1,4-dioxane degradation.

Chuang *et al.* compared an UV/NH$_2$Cl process with UV/chlorine and UV/H$_2$O$_2$ processes on 1,4-dioxane, benzoate, and carbamazepine degradation [124]. The quantum yield

of radical generation by UV photolysis of NH$_2$Cl was 0.20, which was lower than 0.62 for HOCl, 0.55 for ClO$^-$, and 0.5 for H$_2$O$_2$. The degradation performance of UV/NH$_4$Cl was similar to that of UV/H$_2$O$_2$ for three targeted contaminants, and did not depend on pH ranging from 5.5–8.3. At pH 5.5, the UV/chlorine process was the most efficient for all three contaminants. However, the performances of UV/NH$_4$Cl process on benzoate and 1,4-dioxane degradation were superior to those of UV/chlorine process at pH 7.0 and 8.3, likely due to more efficient radical scavenging by ClO$^-$ and HOCl. On the contrary, Wang *et al.* reported that an UV/NH$_2$Cl process was less effective in removing residual organic matter in a used algal medium than UV/H$_2$O$_2$ and UV/S$_2$O$_8^{2-}$ processes [125]. Thus, a process optimization may be required for valid evaluation of the UV/NH$_2$Cl process.

Li *et al.* reported that 1,4-dioxane degradation by a combined process of UV photolysis of NH$_2$Cl and S$_2$O$_8^{2-}$ [84]. In this process excessive NH$_2$Cl consumed HO$^{\cdot}$, SO$_4^{\cdot-}$, and Cl$_2^{\cdot-}$ (reactions (63–65)), which lowered the performance, when the molar ratio of NH$_2$Cl to S$_2$O$_8^{2-}$ was above 0.1. In addition, the process was sensitive to pH due to a disproportionation of NH$_2$Cl at pH<6 into less-photoreactive dichloramine (NHCl$_2$) and radical scavenging by NH$_4^+$ (reactions (66–68)).

$$NH_2Cl + HO^{\cdot} \rightarrow NHCl^{\cdot} + H_2O \ (k_{65} = 5.1 \times 10^8 \ L/(mol \cdot s)) \tag{63}$$

$$NH_2Cl + SO_4^{\cdot-} \rightarrow NHCl^{\cdot} + HSO_4^{-} \ (k_{66} = 2.4 \times 10^7 \ L/(mol \cdot s)) \tag{64}$$

Fig. 8 Reaction pathways of amine radical produced by the photolysis of NH_4Cl. $NH_2^{\cdot}$ and $Cl^{\cdot}$ are primary radicals in UV/NH_2Cl. $Cl_2^{\cdot-}$ and $HO^{\cdot}$ are produced through the reaction scheme in **Fig. 3**. Dashed pathways were assumed by Li *et al.* [84].

$$NH_2Cl + Cl_2^{\cdot-} \rightarrow NHCl^{\cdot} + H^+ + 2Cl^- \quad (k_{67} = 6.5 \times 10^6 \text{ L/(mol·s)}) \tag{65}$$

$$2NH_2Cl \rightarrow NHCl_2 + NH_3 \tag{66}$$

$$NH_4^+ + Cl^{\cdot} \rightarrow NH_2^{\cdot} + 2H^+ + Cl^- \quad (k_{69} = 1.3 \times 10^5 \text{ L/(mol·s)}) \tag{67}$$

$$NH_4^+ + Cl_2^{\cdot-} \rightarrow NH_2^{\cdot} + 2H^+ + 2Cl^- \quad (k_{70} = 1.3 \times 10^5 \text{ L/(mol·s)}) \tag{68}$$

Although Bu *et al.* reported that carbamazepine degradation by an UV/NH_2Cl process did not depend on pH≥6.0 [126], the disproportionation and radical scavenging by NH_2Cl and NH_4^+ are also valid for UV/NH_2Cl processes and will influence the process performance. In addition to pH, HCO_3^- and NOM are reported to be main inhibitors for UV/NH_2Cl processes through radical scavenging effects of HCO_3^- (reactions (43), (45), and (47)) and NOM and UV shielding effect of NOM [126].

UV/ClO$_2$ process

Chlorine dioxide (ClO_2) is an alternative disinfectant for water treatment, whose disinfection mechanism is thought to be disruption of protein synthesis of bacteria [127], which is photolyzed by UV light and produces $ClO^{\cdot}$, $Cl^{\cdot}$, O (^3P), and O_2 as follows:

$$ClO_2 + h\nu \rightarrow ClO^{\cdot} + O(^3P) \tag{69}$$

$$ClO_2 + h\nu \rightarrow Cl^{\cdot} + O_2 \tag{70}$$

The quantum yields of reaction (69) and (70) were reported to be 0.045 and 0.10, respectively [128]. Sichel *et al.* compared UV photolysis of ClO_2 (UV/ClO_2 process) with UV/chlorine and UV/H_2O_2 processes for 8 emerging contaminants [65]. Although the UV/ClO_2 process effectively degraded 17-a-ethinylestradiol, sulfamethoxazole, and dichlofenac, the degradation efficiency was equivalent to or much lower than that of UV/chlorine and UV/H_2O_2 processes. The low quantum yield of ClO_2 for radical production and relatively low reactivity of $ClO^{\cdot}$ compared with $HO^{\cdot}$ and $Cl^{\cdot}$ would result in the lower efficiency of UV/ClO_2 process.

APPLICATIONS

UV/chlorine processes are newcomers in the field of advanced oxidation technologies. Accordingly, their application studies are not abundant very much. Published papers of UV/chlorine AOPs in real samples are listed in **Table 6**. Only 4 researches are performed on a full or pilot scale, and others are done on a lab scale. **Figure 9** shows the specifications of published papers of applied UV/chlorine processes. The most popular application field of UV/chlorine processes is water supply (drinking water + surface water) followed by wastewater treatment. The main target is the removal of organic matter like micropollutants and drinking water related targets of disinfection, DBPs control, and taste and odor control. The concentration level of micropollutants, DBPs, and taste and odor compounds is usually μM-order or less. Therefore, the applied chlorine dose usually remained ≤10 mg-Cl_2/L, whereas 200–300 mg-Cl_2/L of chlorine dose was applied to a solar-UV/chlorine experiment of oil sand process-affected water due to the higher contaminant concentration (21.6 mg/L) [73]. The ratios of chlorine dose to contaminants concentration in literatures were usually ≥10. Thus, the chlorine dose/contaminants ratio of 10 may be a guidepost for UV/chlorine AOPs application. The reported contact time of UV irradiation was widely varied from 6 s to 420 min. However, 6–40 s of contact time was applied in the full and pilot scale experiments [47,48,129]. Since the chlorine dose was relatively low, namely ≤10 mg-Cl_2/L, a short contact time less than 1 min may be enough for UV/chlorine AOPs.

The performance of UV/chlorine AOPs often lowers in real waters. For instance, the degradation rate of carbamazepine in a WWTP effluent was reported to be 29.8% lower than that in ultrapure water [83]. Javier Benitez *et al.* observed that degradation rates of three contaminants was dropped to 52–79% in a surface water and 25–60% in WWTP effluents compared with those in ultrapure water [75]. Dao *et al.* reported that the degradation rate of paracetamol in a tap water and in a surface water was 54 and 67% lower than that in deionized water, respectively, and the lower degradation efficiency of paracetamol in real waters resulted from higher concentrations of NH_4^+, Cl^-, SO_4^{2-}, phosphate, inorganic carbon (e.g. HCO_3^-), and especially DOM [81]. Among various solutes in real waters inorganic carbon and DOM are thought to be responsible for the inhibition effect, which act as radical scavengers and decrease the effective radical concentration available to react with contaminants [75,83]. The latter also acts as oxidant consumer and often absorbs UV radiation, which inhibits the UV photolysis of free chlorine and contaminants by shielding. Other solutes like bromide ion will also inhibit the process as described in INFLUENTIAL FACTORS section, if they are contaminated.

In drinking water related applications the removal of PPCPs and odor compounds of geosmin and 2-methylisoborneol (2-MIB) is discussed by many researchers [20,65,75,129–131]. However, DBPs formation has been also mentioned in the most of researches, because safety is critically important for drinking water. It was reported that DBPs such as THMs, HAAs, HANs, ClO_3^-, and BrO_3^- are produced by UV/chlorine treatment and/or post-chlorination in drinking or surface water [47,56,65,130,131]. However, Sichel *et al.* reported that THMs formation was much lower than the regulation and NDMA formation was not detected, when the residual chlorine after UV/chlorine treatment was quenched [65]. Pisarenko *et al.* also said that THMs formation did not differ from the control [56]. Although HAAs formation was enhanced by UV/chlorine treatment in comparison with chlorination alone, the formation was much lower than the regulation [56]. Full-scale experiments also demonstrated the THMs and HAAs formation by UV/chlorine treatment was similar to that by chlorination alone or UV/H_2O_2 [47]. Watts *et al.* concluded that THMs and HAAs formation is not a problem in an UV/chlorine process at a chlorine dose <10 mg/L and a contact time <1 min [130]. Yang *et al.* investigated the formation potential of THMs, HANs, CH, HKs, and TCNM by post-chlorination after UV/chlorine treatment [131]. As a result, these DBPs formation potential by UV/chlorine treatment was similar to that by UV/H_2O_2 and the control. Thus, it seems that UV/chlorine processes do not enhance the DBPs formation very much. However, Wang *et al.* reported that DCAN and bromochloroacetonitrile were instantaneously produced during UV/chlorine treatment [47]. Therefore, further thorough investigations of DBPs formation may be required for water supply purposes.

CONCLUSIONS

Scientific papers on UV/chlorine AOPs have been rapidly increased from 2016 and their scientific and technological information has been steadily accumulated. In this paper, almost all of published papers on UV/chlorine AOPs are emergently reviewed for understanding the state of the art of these technologies.

The most popular UV/chlorine process is free chlorine photolysis using a low-pressure mercury vapor lamp (LP-UV/chlorine). It is no doubt that HO$^•$ and Cl$^•$ are primary
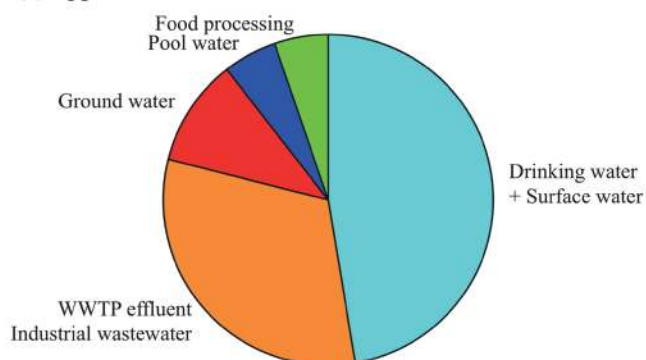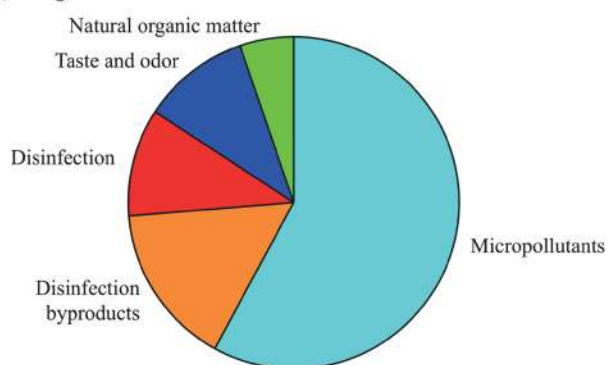
Table 6 Real applications of UV/chlorine AOPs.

Source / Target	Process	Chlorine dose	Performance	Ref.
Tap water / 8 PPCPs (0.1–1 µg/L)	LP-UV/chlorine (lab scale)	1–6 mg-Cl_2/L	EE/O: 0.16 kWh/(m^3·order) for carbamazepine	[65]
Post-filtration water in a DWTP	LP-UV/chlorine (lab scale)	8–10 mg-Cl_2/L	THM and HAA formation < 10 µg/L	[130]
Post-filtration water in DWTPs / 10 PPCPs (100 ng/L)	LP-UV/chlorine (lab scale)	3–5 mg-Cl_2/L	27–99% removal. Not significant in enhancement of DBP formation	[131]
Tap water and surface water / pracetamol (10 µM)	LP-UV/chlorine (lab scale)	100 µM	Relative degradation rate against in deionized water: 46% in tap water, 33% in surface water	[81]
Influent, sand filtered water, and GAC filtered water in a DWTP / carbamazepine (5 µM)	LP-UV/NH_2Cl (lab scale)	70 µM	EE/O: 2.3–3.2 kWh/(m^3·order). Relative degradation rate against deionized water: 18% in influent, 22% in sand filtered water, 54% in GAC filtered water	[126]
Surface water / natural organic matter (NOM)	UV/electro-generated chlorine (lab scale)	2–10 mg-Cl_2/L	SUVA reduction: 62.8–91.5% in UV-C and 44.2–72.3% in UV-A	[56]
Surface water / geosmin (18–400 ng/L), 2-MIB (20 µg/L)	MP-UV/chlorine (full and pilot scale)	2–10 mg-Cl_2/L	EE/O [kWh/(m^3·order)]: 0.16–0.65 for geosmine, 0.22–1.0 for 2-MIB	[129]
Surface water	MP-UV/chlorine (full and pilot scale)	2–10 mg-Cl_2/L	Minimal THM, HAA, HAN, and AOX formation at 10 mg-Cl_2/L	[47]
Surface water and WWTP effluent / amitriptyline, methyl salicylate, 2-phenoxyethanol (1 µM)	LP-UV/chlorine (lab scale)	10 µM	Relative degradation rate against in ultrapure water: 52–79% in surface water, 25–60% in WWTP effluent	[75]
WWTP effluent / carbamazepine (8.5 µM)	LP-UV/chlorine (lab scale)	0.14–0.56 mM	Degradation rate in WWTP effluent: 70.2% of that in ultrapure water	[83]
WWTP effluent / 28 PPCPs (1 µg/L)	LP-UV/chlorine (lab scale)	50 µM	EE/O: 19.1–98.1% lower than those of UV/H_2O_2 without ronidazole (0.06–4.5 kWh/(m^3·order))	[117]
WWTP effluent / 16 emerging contaminants (0.03–2.55 µg/L)	MP-UV/chlorine (pilot scale)	3–6 mg-Cl_2/L	Superior to UV/H_2O_2 in removal efficiency. >97% removal of total estrogenic activity at 5 or 6 mg-Cl_2/L	[48]
WWTP effluent / *Bacillus subtilis* spore	UV-LED/chlorine (lab scale)	6.6–6.8 mg-Cl_2/L	Inactivation rate: 1.8–2.3 times higher than chlorination. 64–67% of inactivation rate in a sterile phosphate buffer	[68]
Oil sand process-affected water / naphthenic acids (21.6 mg/L)	solar-UV/chlorine (lab scale)	200–300 mg-ClO^-/L	76–84% removal	[73]

Table 6 Real applications of UV/chlorine AOPs. *(continued)*

Source / Target	Process	Chlorine dose	Performance	Ref.
Ground water / TCE (8–15 µg/L), NDMA (27–1300 ng/L)	MP-UV/chlorine (pilot scale)	0.8–7.7 mg-Cl_2/L	Residual conc.: <0.5–2.9 mg/L in TCE, <2 ng/L in NDMA	[143]
Ground water / MTBE (1000 µg/L)	LP-UV/chlorine and MP-UV/chlorine (lab scale)	5–10 mg-Cl_2/L	EE/O: 4.01 kWh/(m^3·order) for LP-UV/chlorine, 54.67 kWh/(m^3·order) for MP-UV/chlorine	[106]
Pool water	LP-UV/free and combined chlorine (lab scale)	0.4–0.5 mg-Cl_2/L	Slightly increase in NDMA formation (ca. 0.02 nM)	[64]
Wild blueberry / bacterial flora	LP-UV/chlorine (lab scale)	92 mg-Cl_2/g	No synergistic effect	[71]

AOX: adsorbable organic halide, DBP, disinfection byproduct, DWTP: drinking water treatment plant, EE/O: electric energy per an order reduction of pollutant, HAA: haloacetic acid, HAN: haloacetonitrile, 2-MIB: 2-methylisoboruneol, MTBE: methyl tertiary butyl ether, TCE: trichloroethylene, NDMA: nitrosodimethylamine, THM: trihalomethane, SUVA: specific UV absorbance, WWTP: wastewater treatment plant

Fig. 9 Specifications of application of UV/chlorine processes to real samples.

chemical equilibriums and radical chain reactions take part in oxidative degradation of pollutants, and in some cases contributions of secondary radicals are mainly responsible for pollutants degradation in UV/chlorine system. Accordingly, understandings of reactivity of RCS with target pollutants will be required for an effective application of this technology to actual water treatment. Since RCS are produced in UV/chlorine system, unfavorable byproducts formation is apprehended. There are many reports on DBPs formation during UV/chlorine processes. Part of them showed the increase in DBPs formation during UV/chlorine treatment but others demonstrated the reverse results. However, based on application researches in real waters, it seems that UV/chlorine AOPs do not enhance DBPs formation very much in comparison with chlorination, when the processes are optimized. The performance of UV/chlorine AOPs are influenced by pH, chlorine dose, halide ions, alkalinity, and NOM. Alkalinity and NOM is common inhibitors for AOPs, and UV/chlorine AOPs receive negative impacts by them too. Acidic pH is usually favorable to UV/chlorine AOPs due to three mechanisms: a change in quantum yield of chlorine photolysis, equilibrium shifts of radical species, and a higher radical scavenging effect of ClO^- than that of HOCl. The influence of halide ions depends on the reactivity of secondary radicals with target pollutants. In most cases, bromide ion contamination deteriorates the advanced oxidation performance due to less reactivity of bromine-based radicals than that of RCS. Comparative studies revealed that UV/chlorine AOPs are usually more energy-efficient than UV/H_2O_2 and $UV/S_2O_8^{2-}$ processes, especially when UV/chlorine AOPs are operated under acidic conditions. In addition to LP-UV/chlorine, various process derivatives have been developed,

radicals produced by the UV photolysis of free chlorine. However, the advanced oxidation effect of UV/chlorine processes is not necessarily owing to these radicals alone. Secondary radicals such as $Cl_2^{·-}$ and $ClO^·$ produced through

which introduce a substitute light source like MP-UV, ex-cimer-UV, UV-LED, and solar radiation, an onsite chlorine production system using electrolysis, or a chlorine substitute like NH_2Cl and ClO_2 into the UV/chlorine system. The de-rivatives are expected to expand the application area of UV/chlorine AOPs.

In conclusion, UV/chlorine processes are promising AOPs in their potential abilities on pollutants degradation, higher energy efficiencies, and a low barrier to their installation in practical processes due to well-established unit operations of UV irradiation and chlorination, whereas DBPs forma-tion should be checked prior to each practical application. Furthermore, it is desired to develop and optimize a whole process combined with other unit processes for maximizing benefits in water treatment in the future.

ACKNOWLEDGEMENTS

SUPPLEMENTARY MATERIALS

Supplementary Materials for this article are available on the journal website in a separate file.

https://www.jstage.jst.go.jp/article/jwet/17/5/17_19-021/_supplement/_download/17_19-021_1.pdf

REFERENCES

[1] Glaze WH, Kang JW, Chapin DH: The chemistry of water treatment processes involving ozone, hydrogen peroxide and ultraviolet radiation. *Ozone Sci. Eng.*, **9**(4), 335–352, 1987. doi:10.1080/01919518708552148

[2] Suty H, De Traversay C, Cost M: Applications of ad-vanced oxidation processes: present and future. *Water Sci. Technol.*, **49**(4), 227–233, 2004. PMID:15077976 doi:10.2166/wst.2004.0270

[3] Wisniak J: The history of chlorine–From discovery to commodity. *Indian J. Chem. Technol.*, **9**, 450–463, 2002.

[4] Lemay P, Oesper RE: Claude Louis Berthollet (1748-1822). *J. Chem. Educ.*, **23**(4), 158, 1946. doi:10.1021/ed023p158

[5] Kishimoto N, Nishimura H: Effect of pH and molar ratio of pollutant to oxidant on a photochemical ad-vanced oxidation process using hypochlorite. *Environ. Technol.*, **36**(19), 2436–2442, 2015. PMID:25809495 doi:10.1080/09593330.2015.1034187

[6] Hewitt PC: Induction vapor or gas electric lamp. No. 843533, United States Patent Office, 1907.

[7] Allmand AJ, Cunliffe PW, Maddison REW: CXVII.—The photodecomposition of chlorine water and of aqueous hypochlorous acid solutions. Part I. *J. Chem. Soc. Trans.*, **127**(0), 822–840, 1925. doi:10.1039/CT9252700822

[8] Allmand AJ, Cunliffe PW, Maddison REW: C.—The photodecomposition of chlorine water and of aqueous hypochlorous acid solutions. Part II. *J. Chem. Soc.*, 655–669, 1927. doi:10.1039/JR9270000655

[9] Young KW, Allmand AJ: Experiments on the photoly-sis of aqueous solutions of chlorine, hypochlorous acid, and sodium hypochlorite. *Can. J. Res.*, **27b**(4), 318–331, 1949. doi:10.1139/cjr49b-034

[10] Thomsen CL, Madsen D, Poulsen JA, Thøgersen J, Jensen SJK, Keiding SR: Femtosecond photolysis of aqueous HOCl. *J. Chem. Phys.*, **115**(20), 9361–9369, 2001. doi:10.1063/1.1413964

[11] Madsen D, Thomsen CL, Poulsen JA, Knak Jensen SJ, Thøgersen J, Keiding SR, Krissinel EB: Femtosecond photolysis of HOCl(aq): dissipation of fragment kinetic energy. *J. Phys. Chem. A*, **107**(19), 3606–3611, 2003. doi:10.1021/jp026968u

[12] Buxton GV, Subhani MS: Radiation chemistry and photochemistry of oxychlorine ions. Part 2.—Photode-composition of aqueous solutions of hypochlorite ions. *J. Chem. Soc. Faraday Trans. 1 Phys. Chem. Condens. Phases*, **68**, 958–969, 1972. doi:10.1039/f19726800958

[13] Luňák S, Sedlák P: Photoinitiated reactions of hy-drogen peroxide in the liquid phase. *J. Photochem. Photobiol. Chem.*, **68**(1), 1–33, 1992. doi:10.1016/1010-6030(92)85014-L

[14] Peyton GR, Glaze WH: Destruction of pollutants in water with ozone in combination with ultraviolet radiation. 3. Photolysis of aqueous ozone. *Environ. Sci. Technol.*, **22**(7), 761–767, 1988. PMID:22195658 doi:10.1021/es00172a003

[15] Wardman P: Reduction potentials of one-electron couples involving free radicals in aqueous solution. *J. Phys. Chem. Ref. Data*, **18**(4), 1637–1755, 1989. doi:10.1063/1.555843

[16] Fang J, Fu Y, Shang C: The roles of reactive species in micropollutant degradation in the UV/free chlorine system. *Environ. Sci. Technol.*, **48**(3), 1859–1868, 2014. PMID:24400681 doi:10.1021/es4036094

[17] Huie RE, Clifton CL, Neta P: Electron transfer reaction rates and equilibria of the carbonate and sulfate radical anions. *Int. J. Radiat. Appl. Instrumentation. Part C. Radiat. Phys. Chem.*, **38**(5), 477–481, 1991. doi:10.1016/1359-0197(91)90065-A

[18] Alfassi ZB, Huie RE, Mosseri S, Neta P: Kinetics of one-electron oxidation by the ClO radical. *Int. J. Radiat. Appl. Instrumentation. Part C. Radiat. Phys. Chem.*, **32**(1), 85–88, 1988. doi:10.1016/1359-0197(88)90018-5

[19] Kishimoto N, Katayama Y, Kato M, Otsu H: Technical feasibility of UV/electro-chlorine advanced oxidation process and pH response. *Chem. Eng. J.*, **334**, 2363–2372, 2018. doi:10.1016/j.cej.2017.11.108

[20] Xiang Y, Fang J, Shang C: Kinetics and pathways of ibuprofen degradation by the UV/chlorine advanced oxidation process. *Water Res.*, **90**, 301–308, 2016. PMID:26748208 doi:10.1016/j.watres.2015.11.069

[21] Wu Z, Fang J, Xiang Y, Shang C, Li X, Meng F, Yang X: Roles of reactive chlorine species in trimethoprim degradation in the UV/chlorine process: Kinetics and transformation pathways. *Water Res.*, **104**, 272–282, 2016. PMID:27544349 doi:10.1016/j.watres.2016.08.011

[22] Dong H, Qiang Z, Hu J, Qu J: Degradation of chloramphenicol by UV/chlorine treatment: Kinetics, mechanism and enhanced formation of halonitromethanes. *Water Res.*, **121**, 178–185, 2017. PMID:28527979 doi:10.1016/j.watres.2017.05.030

[23] Guo K, Wu Z, Shang C, Yao B, Hou S, Yang X, Song W, Fang J: Radical chemistry and structural relationships of PPCP degradation by UV/chlorine treatment in simulated drinking water. *Environ. Sci. Technol.*, **51**(18), 10431–10439, 2017. PMID:28809556 doi:10.1021/acs.est.7b02059

[24] Buxton GV, Greenstock CL, Helman WP, Ross AB: Critical Review of rate constants for reactions of hydrated electrons, hydrogen atoms and hydroxyl radicals ($\cdot$OH/$\cdot$O$^-$ in Aqueous Solution. *J. Phys. Chem. Ref. Data*, **17**(2), 513–886, 1988. doi:10.1063/1.555805

[25] Neta P, Huie RE, Ross AB: Rate constants for reactions of inorganic radicals in aqueous solution. *J. Phys. Chem. Ref. Data*, **17**(3), 1027–1284, 1988. doi:10.1063/1.555808

[26] Buxton GV, Bydder M, Arthur Salmon G: Reactivity of chlorine atoms in aqueous solution Part 1The equilibrium Cl^{MNsbd}+Cl$^-$Cl$_2^-$. *J. Chem. Soc., Faraday Trans.*, **94**(5), 653–657, 1998. doi:10.1039/a707377a

[27] Patton S, Li W, Couch KD, Mezyk SP, Ishida KP, Liu H: Impact of the ultraviolet photolysis of monochloramine on 1,4-dioxane removal: New insights into potable water reuse. *Environ. Sci. Technol. Lett.*, **4**(1), 26–30, 2017. doi:10.1021/acs.estlett.6b00444

[28] Alegre L, Gerone M, Rosso JA, Bertolotti SG, Braun AM, Mártire DO, Gonzalez MC: Kinetic study of the reactions of chlorine atoms and Cl$_2^{\cdot-}$ radical anions in aqueous solutions. 1. Reaction with benzene. *J. Phys. Chem. A*, **104**(14), 3117–3125, 2000. doi:10.1021/jp9929768

[29] Watts MJ, Linden KG: Chlorine photolysis and subsequent OH radical production during UV treatment of chlorinated water. *Water Res.*, **41**(13), 2871–2878, 2007. PMID:17498769 doi:10.1016/j.watres.2007.03.032

[30] Minakata D, Kamath D, Maetzold S: Mechanistic insight into the reactivity of chlorine-derived radicals in the aqueous-phase UV–Chlorine advanced oxidation process: Quantum mechanical calculations. *Environ. Sci. Technol.*, **51**(12), 6918–6926, 2017. PMID:28541663 doi:10.1021/acs.est.7b00507

[31] Wu Z, Guo K, Fang J, Yang X, Xiao H, Hou S, Kong X, Shang C, Yang X, Meng F, Chen L: Factors affecting the roles of reactive species in the degradation of micropollutants by the UV/chlorine process. *Water Res.*, **126**, 351–360, 2017. PMID:28985600 doi:10.1016/j.watres.2017.09.028

[32] Buxton GV, Bydder M, Salmon GA, Williams JE: The reactivity of chlorine atoms in aqueous solution. Part III. The reactions of Cl$\bullet$ with solutes. *Phys. Chem. Chem. Phys.*, **2**(2), 237–245, 2000. doi:10.1039/a907133d

[33] Schmidt MW, Baldridge KK, Boatz JA, Elbert ST, Gordon MS, Jensen JH, Koseki S, Matsunaga N, Nguyen KA, Su S, Windus TL, Dupuis M, Montgomery JA: General atomic and molecular electronic structure system. *J. Comput. Chem.*, **14**(11), 1347–1363, 1993. doi:10.1002/jcc.540141112

[34] Minakata D, Li K, Westerhoff P, Crittenden J: Development of a group contribution method to predict aqueous phase hydroxyl radical (HO$\bullet$) reaction rate constants. *Environ. Sci. Technol.*, **43**(16), 6220–6227, 2009. PMID:19746717 doi:10.1021/es900956c

[35] Ezell MJ, Wang W, Ezell AA, Soskin G, Finlayson-Pitts BJ: Kinetics of reactions of chlorine atoms with a series of alkenes at 1 atm and 298 K: structure and reactivity. *Phys. Chem. Chem. Phys.*, **4**(23), 5813–5820, 2002. doi:10.1039/b207529f

[36] Hasegawa K, Neta P: Rate constants and mechanisms of reaction of chloride (Cl_2^-) radicals. *J. Phys. Chem.*, **82**(8), 854–857, 1978. doi:10.1021/j100497a003

[37] Kong X, Wu Z, Ren Z, Guo K, Hou S, Hua Z, Li X, Fang J: Degradation of lipid regulators by the UV/chlorine process: Radical mechanisms, chlorine oxide radical (ClO$^\bullet$)-mediated transformation pathways and toxicity changes. *Water Res.*, **137**, 242–250, 2018. PMID:29550727 doi:10.1016/j.watres.2018.03.004

[38] Minakata D, Crittenden J: Linear free energy relationships between aqueous phase hydroxyl radical reaction rate constants and free energy of activation. *Environ. Sci. Technol.*, **45**(8), 3479–3486, 2011. PMID:21410278 doi:10.1021/es1020313

[39] Kamath D, Minakata D: Emerging investigators series: ultraviolet and free chlorine aqueous-phase advanced oxidation process: kinetic simulations and experimental validation. *Environ. Sci. Water Res. Technol.*, **4**(9), 1231–1238, 2018. doi:10.1039/C8EW00196K

[40] Pan M, Wu Z, Tang C, Guo K, Cao Y, Fang J: Emerging investigators series: comparative study of naproxen degradation by the UV/chlorine and the UV/H_2O_2 advanced oxidation processes. *Environ. Sci. Water Res. Technol.*, **4**(9), 1219–1230, 2018. doi:10.1039/C8EW00105G

[41] Henze M, Ledin A: Types, characteristics and quantities of classic, combined domestic wastewaters. In: Lens P, Zeeman G, Lettinga G (eds): Decentralised Sanitation and Reuse Concepts, Systems and Implementation, IWA Publishing, London, pp. 57–72, 2001.

[42] Adam LC, Gordon G: Hypochlorite Ion Decomposition: Effects of Temperature, Ionic Strength, and Chloride Ion. *Inorg. Chem.*, **38**(6), 1299–1304, 1999. PMID:11670917 doi:10.1021/ic980020q

[43] Azizi O, Hubler D, Schrader G, Farrell J, Chaplin BP: Mechanism of perchlorate formation on boron-doped diamond film anodes. *Environ. Sci. Technol.*, **45**(24), 10582–10590, 2011. PMID:22029642 doi:10.1021/es202534w

[44] Kang N, Anderson TA, Rao B, Jackson WA: Characteristics of perchlorate formation via photodissociation of aqueous chlorite. *Environ. Chem.*, **6**(1), 53, 2009. doi:10.1071/EN08094

[45] Rao B, Estrada N, McGee S, Mangold J, Gu B, Jackson WA: Perchlorate production by photodecomposition of aqueous chlorine solutions. *Environ. Sci. Technol.*, **46**(21), 11635–11643, 2012. PMID:22962844 doi:10.1021/es3015277

[46] Feng Y, Smith DW, Bolton JR: A potential new method for determination of the fluence (UV dose) delivered in UV reactors involving the photodegradation of free chlorine. *Water Environ. Res.*, **82**(4), 328–334, 2010. PMID:20432650 doi:10.2175/106143009X447920

[47] Wang D, Bolton JR, Andrews SA, Hofmann R: Formation of disinfection by-products in the ultraviolet/chlorine advanced oxidation process. *Sci. Total Environ.*, **518-519**, 49–57, 2015. PMID:25747363 doi:10.1016/j.scitotenv.2015.02.094

[48] Rott E, Kuch B, Lange C, Richter P, Kugele A, Minke R: Removal of Emerging Contaminants and Estrogenic Activity from Wastewater Treatment Plant Effluent with UV/Chlorine and UV/H_2O_2 Advanced Oxidation Treatment at Pilot Scale. *Int. J. Environ. Res. Public Health*, **15**(5), 935, 2018. PMID:29735959 doi:10.3390/ijerph15050935

[49] Boorman GA, Dellarco V, Dunnick JK, Chapin RE, Hunter S, Hauchman F, Gardner H, Cox M, Sills RC: Drinking water disinfection byproducts: review and approach to toxicity evaluation. *Environ. Health Perspect.*, **107**(Suppl 1): 207–217, 1999. PMID:10229719 PMID:10229719 doi:10.1289/ehp.99107s1207

[50] Krasner SW, Weinberg HS, Richardson SD, Pastor SJ, Chinn R, Sclimenti MJ, Onstad GD, Thruston AD: Occurrence of a new generation of disinfection byproducts. *Environ. Sci. Technol.*, **40**(23), 7175–7185, 2006. PMID:17180964 doi:10.1021/es060353j

[51] Zhou S, Xia Y, Li T, Yao T, Shi Z, Zhu S, Gao N: Degradation of carbamazepine by UV/chlorine advanced oxidation process and formation of disinfection by-products. *Environ. Sci. Pollut. Res. Int.*, **23**(16), 16448–16455, 2016. PMID:27164884 doi:10.1007/s11356-016-6823-x

[52] Gao ZC, Lin YL, Xu B, Pan Y, Xia SJ, Gao NY, Zhang TY, Chen M: Degradation of acrylamide by the UV/chlorine advanced oxidation process. *Chemosphere*, **187**, 268–276, 2017. PMID:28854381 doi:10.1016/j.chemosphere.2017.08.085

[53] Huang N, Wang T, Wang WL, Wu QY, Li A, Hu HY: UV/chlorine as an advanced oxidation process for the degradation of benzalkonium chloride: Synergistic effect, transformation products and toxicity evaluation. *Water Res.*, **114**, 246–253, 2017.   PMID:28254642   doi:10.1016/j.watres.2017.02.015

[54] Zhu Y, Wu M, Gao N, Chu W, Li K, Chen S: Degradation of phenacetin by the UV/chlorine advanced oxidation process: Kinetics, pathways, and toxicity evaluation. *Chem. Eng. J.*, **335**, 520–529, 2018.   doi:10.1016/j.cej.2017.10.070

[55] Xiang H, Shao Y, Gao N, Lu X, An N, Tan C, Zheng Z: Degradation of diuron by chlorination and UV/chlorine process: Degradation kinetics and the formation of disinfection by-products. *Separ. Purif. Tech.*, **202**, 365–372, 2018.   doi:10.1016/j.seppur.2018.03.073

[56] Pisarenko AN, Stanford BD, Snyder SA, Rivera SB, Boal AK: Investigation of the use of Chlorine Based Advanced Oxidation in Surface Water: Oxidation of Natural Organic Matter and Formation of Disinfection Byproducts. *Journal of Advanced Oxidation Technologies*, **16**(1), 137–150, 2013.   doi:10.1515/jaots-2013-0115

[57] Lu X, Shao Y, Gao N, Chen J, Deng H, Chu W, An N, Peng F: Investigation of clofibric acid removal by UV/persulfate and UV/chlorine processes: Kinetics and formation of disinfection byproducts during subsequent chlor(am)ination. *Chem. Eng. J.*, **331**, 364–371, 2018.   doi:10.1016/j.cej.2017.08.117

[58] Deborde M, von Gunten U: Reactions of chlorine with inorganic and organic compounds during water treatment—Kinetics and mechanisms: A critical review. *Water Res.*, **42**(1-2), 13–51, 2008.   PMID:17915284   doi:10.1016/j.watres.2007.07.025

[59] Weng S, Blatchley ER III: Ultraviolet-induced effects on chloramine and cyanogen chloride formation from chlorination of amino acids. *Environ. Sci. Technol.*, **47**(9), 4269–4276, 2013.   PMID:23560482   doi:10.1021/es400273w

[60] Deng L, Huang CH, Wang YL: Effects of combined UV and chlorine treatment on the formation of trichloronitromethane from amine precursors. *Environ. Sci. Technol.*, **48**(5), 2697–2705, 2014.   PMID:24475954   doi:10.1021/es404116n

[61] Krasner SW, Mitch WA, McCurry DL, Hanigan D, Westerhoff P: Formation, precursors, control, and occurrence of nitrosamines in drinking water: A review. *Water Res.*, **47**(13), 4433–4450, 2013.   PMID:23764594   doi:10.1016/j.watres.2013.04.050

[62] Pehlivanoglu-Mantas E, Sedlak DL: Measurement of dissolved organic nitrogen forms in wastewater effluents: Concentrations, size distribution and NDMA formation potential. *Water Res.*, **42**(14), 3890–3898, 2008.   PMID:18672263   doi:10.1016/j.watres.2008.05.017

[63] Yang L, Chen Z, Shen J, Xu Z, Liang H, Tian J, Ben Y, Zhai X, Shi W, Li G: Reinvestigation of the nitrosamine-formation mechanism during ozonation. *Environ. Sci. Technol.*, **43**(14), 5481–5487, 2009.   PMID:19708385   doi:10.1021/es900319f

[64] Soltermann F, Lee M, Canonica S, von Gunten U: Enhanced N-nitrosamine formation in pool water by UV irradiation of chlorinated secondary amines in the presence of monochloramine. *Water Res.*, **47**(1), 79–90, 2013.   PMID:23098367   doi:10.1016/j.watres.2012.09.034

[65] Sichel C, Garcia C, Andre K: Feasibility studies: UV/chlorine advanced oxidation treatment for the removal of emerging contaminants. *Water Res.*, **45**(19), 6371–6380, 2011.   PMID:22000058   doi:10.1016/j.watres.2011.09.025

[66] Stefan MI, Bolton JR: UV Direct Photolysis of *N*-Nitrosodimethylamine (NDMA): Kinetic and Product Study. *Helv. Chim. Acta*, **85**(5), 1416, 2002.   doi:10.1002/1522-2675(200205)85:5<1416::AID-HLCA1416>3.0.CO;2-I

[67] Rattanakul S, Oguma K, Sakai H, Takizawa S: Inactivation of viruses by combination processes of UV and chlorine. *J. Water Environ. Technol.*, **12**(6), 511–523, 2014.   doi:10.2965/jwet.2014.511

[68] Li GQ, Huo ZY, Wu QY, Lu Y, Hu HY: Synergistic effect of combined UV-LED and chlorine treatment on Bacillus subtilis spore inactivation. *Sci. Total Environ.*, **639**, 1233–1240, 2018.   PMID:29929290   doi:10.1016/j.scitotenv.2018.05.240

[69] Zhou P, Di Giovanni GD, Meschke JS, Dodd MC: Enhanced inactivation of *Cryptosporidium parvum* oocysts during solar photolysis of free available chlorine. *Environ. Sci. Technol. Lett.*, **1**(11), 453–458, 2014.   doi:10.1021/ez500270u

[70] Sun J, Bu L, Deng L, Shi Z, Zhou S: Removal of *Microcystis aeruginosa* by UV/chlorine process: Inactivation mechanism and microcystins degradation. *Chem. Eng. J.*, **349**, 408–415, 2018.   doi:10.1016/j.cej.2018.05.116

[71] Crowe KM, Bushway AA, Bushway RJ, Davis-Dentici K, Hazen RA: A comparison of single oxidants versus advanced oxidation processes as chlorine-alternatives for wild blueberry processing (*Vaccinium angustifolium*). *Int. J. Food Microbiol.*, **116**(1), 25–31, 2007. PMID:17350128 doi:10.1016/j.ijfoodmicro.2006.12.027

[72] Hurwitz G, Pornwongthong P, Mahendra S, Hoek EMV: Degradation of phenol by synergistic chlorine-enhanced photo-assisted electrochemical oxidation. *Chem. Eng. J.*, **240**, 235–243, 2014. doi:10.1016/j.cej.2013.11.087

[73] Shu Z, Li C, Belosevic M, Bolton JR, El-Din MG: Application of a solar UV/chlorine advanced oxidation process to oil sands process-affected water remediation. *Environ. Sci. Technol.*, **48**(16), 9692–9701, 2014. PMID:25051215 doi:10.1021/es5017558

[74] Yin K, Deng Y, Liu C, He Q, Wei Y, Chen S, Liu T, Luo S: Kinetics, pathways and toxicity evaluation of neonicotinoid insecticides degradation via UV/chlorine process. *Chem. Eng. J.*, **346**, 298–306, 2018. doi:10.1016/j.cej.2018.03.168

[75] Javier Benitez F, Real FJ, Acero JL, Casas F: Assessment of the UV/Cl$_2$ advanced oxidation process for the degradation of the emerging contaminants amitriptyline hydrochloride, methyl salicylate and 2-phenoxyethanol in water systems. *Environ. Technol.*, **38**(20), 2508–2516, 2017. PMID:27927078 doi:10.1080/09593330.2016.1269836

[76] Wang AQ, Lin YL, Xu B, Hu CY, Xia SJ, Zhang TY, Chu WH, Gao NY: Kinetics and modeling of iodoform degradation during UV/chlorine advanced oxidation process. *Chem. Eng. J.*, **323**, 312–319, 2017. doi:10.1016/j.cej.2017.04.061

[77] Watts MJ, Rosenfeldt EJ, Linden KG: Comparative OH radical oxidation using UV-Cl$_2$ and UV-H$_2$O$_2$ processes. *J. Water Supply*, **56**(8), 469–477, 2007. doi:10.2166/aqua.2007.028

[78] Qin L, Lin YL, Xu B, Hu CY, Tian FX, Zhang TY, Zhu WQ, Huang H, Gao NY: Kinetic models and pathways of ronidazole degradation by chlorination, UV irradiation and UV/chlorine processes. *Water Res.*, **65**, 271–281, 2014. PMID:25141357 doi:10.1016/j.watres.2014.07.041

[79] Fang J, Liu J, Shang C, Fan C: Degradation investigation of selected taste and odor compounds by a UV/chlorine advanced oxidation process. *Int. J. Environ. Res. Public Health*, **15**(2), 284, 2018. PMID:29414884 doi:10.3390/ijerph15020284

[80] Kumar K, Margerum DW: Kinetics and mechanism of general-acid-assisted oxidation of bromide by hypochlorite and hypochlorous acid. *Inorg. Chem.*, **26**(16), 2706–2711, 1987. doi:10.1021/ic00263a030

[81] Dao Y, Tran H, Tran-Lam T, Pham T, Le G: Degradation of Paracetamol by an UV/Chlorine Advanced Oxidation Process: Influencing Factors, Factorial Design, and Intermediates Identification. *Int. J. Environ. Res. Public Health*, **15**(12), 2637, 2018. PMID:30477263 doi:10.3390/ijerph15122637

[82] Chan PY, Gamal El-Din M, Bolton JR: A solar-driven UV/Chlorine advanced oxidation process. *Water Res.*, **46**(17), 5672–5682, 2012. PMID:22939221 doi:10.1016/j.watres.2012.07.047

[83] Wang WL, Wu QY, Huang N, Wang T, Hu HY: Synergistic effect between UV and chlorine (UV/chlorine) on the degradation of carbamazepine: Influence factors and radical species. *Water Res.*, **98**, 190–198, 2016. PMID:27105033 doi:10.1016/j.watres.2016.04.015

[84] Li W, Patton S, Gleason JM, Mezyk SP, Ishida KP, Liu H: UV Photolysis of Chloramine and Persulfate for 1,4-Dioxane Removal in Reverse-Osmosis Permeate for Potable Water Reuse. *Environ. Sci. Technol.*, **52**(11), 6417–6425, 2018. PMID:29653056 doi:10.1021/acs.est.7b06042

[85] Kong X, Jiang J, Ma J, Yang Y, Liu W, Liu Y: Degradation of atrazine by UV/chlorine: Efficiency, influencing factors, and products. *Water Res.*, **90**, 15–23, 2016. PMID:26724435 doi:10.1016/j.watres.2015.11.068

[86] Wu Q, Li Y, Wang W, Wang T, Hu H: Removal of C.I. Reactive Red 2 by low pressure UV/chlorine advanced oxidation. *J. Environ. Sci. (China)*, **41**, 227–234, 2016. PMID:26969069 doi:10.1016/j.jes.2015.06.013

[87] Buxton GV, Dainton FS: The radiolysis of aqueous solutions of oxybromine compounds; the spectra and reactions of BrO and BrO$_2$. *Proc. R. Soc. A Math. Phys. Eng. Sci.*, **304**(1479), 427–439, 1968. doi:10.1098/rspa.1968.0095

[88] Kläning UK, Wolff T: Laser flash photolysis of HCIO, CIO$^-$, HBrO, and BrO$^-$ in aqueous solution. Reactions of Cl- and Br-atoms. *Berichte der Bunsengesellschaft für Phys. Chemie*, **89**(3), 243–245, 1985. doi:10.1002/bbpc.19850890309

[89] National Institute of Standards and Technology: NDRL/NIST Solution Kinetics Database on the Web., 2002. https://kinetics.nist.gov/solution/ [accessed on December 1, 2018]

[90] Zehavi D, Rabani J: Oxidation of aqueous bromide ions by hydroxyl radicals. Pulse radiolytic investigation. *J. Phys. Chem.*, **76**(3), 312–319, 1972. doi:10.1021/j100647a006

[91] Wang Z, Lin YL, Xu B, Xia SJ, Zhang TY, Gao NY: Degradation of iohexol by UV/chlorine process and formation of iodinated trihalomethanes during post-chlorination. *Chem. Eng. J.*, **283**, 1090–1096, 2016. doi:10.1016/j.cej.2015.08.043

[92] Zhao Q, Shang C, Zhang X: Effects of bromide on UV/chlorine advanced oxidation process. *Water Sci. Technol. Water Supply*, **9**(6), 627–634, 2009. doi:10.2166/ws.2009.679

[93] Cheng S, Zhang X, Yang X, Shang C, Song W, Fang J, Pan Y: The Multiple role of bromide ion in PPCPs degradation under UV/chlorine treatment. *Environ. Sci. Technol.*, **52**(4), 1806–1816, 2018. PMID:29338220 doi:10.1021/acs.est.7b03268

[94] Zhang X, He J, Xiao S, Yang X: Elimination kinetics and detoxification mechanisms of microcystin-LR during UV/Chlorine process. *Chemosphere*, **214**, 702–709, 2019. PMID:30293023 doi:10.1016/j.chemosphere.2018.09.162

[95] Fang J, Zhao Q, Fan C, Shang C, Fu Y, Zhang X: Bromate formation from the oxidation of bromide in the UV/chlorine process with low pressure and medium pressure UV lamps. *Chemosphere*, **183**, 582–588, 2017. PMID:28570902 doi:10.1016/j.chemosphere.2017.05.136

[96] Mertens R, von Sonntag C: Photolysis (λ = 354 nm of tetrachloroethene in aqueous solutions. *J. Photochem. Photobiol. Chem.*, **85**(1-2), 1–9, 1995. doi:10.1016/1010-6030(94)03903-8

[97] Matthew BM, Anastasio C: A chemical probe technique for the determination of reactive halogen species in aqueous solution: Part 1 – bromide solutions. *Atmos. Chem. Phys.*, **6**(9), 2423–2437, 2006. doi:10.5194/acp-6-2423-2006

[98] Hudson N, Baker A, Reynolds D: Fluorescence analysis of dissolved organic matter in natural, waste and polluted waters—a review. *River Res. Appl.*, **23**(6), 631–649, 2007. doi:10.1002/rra.1005

[99] Chen J, Gu B, LeBoeuf EJ, Pan H, Dai S: Spectroscopic characterization of the structural and functional properties of natural organic matter fractions. *Chemosphere*, **48**(1), 59–68, 2002. PMID:12137058 doi:10.1016/S0045-6535(02)00041-3

[100] Green SA, Blough NV: Optical absorption and fluorescence properties of chromophoric dissolved organic matter in natural waters. *Limnol. Oceanogr.*, **39**(8), 1903–1916, 1994. doi:10.4319/lo.1994.39.8.1903

[101] Heering W: UV sources − Basics, propertirs and applications. *IUVA News*, **6**(4), 7–13, 2004.

[102] Schalk S, Adam V, Arnold E, Brieden K, Voronov A, Witzke HD: UV-lamps for disinfection and advanced oxidation − Lamp types, technologies and applications. *IUVA News*, **8**(1), 32–37, 2006.

[103] Li M, Qiang Z, Hou P, Bolton JR, Qu J, Li P, Wang C: VUV/UV/chlorine as an enhanced advanced oxidation process for organic pollutant removal from water: Assessment with a novel mini-fluidic VUV/UV photoreaction system (MVPS). *Environ. Sci. Technol.*, **50**(11), 5849–5856, 2016. PMID:27187747 doi:10.1021/acs.est.6b00133

[104] Li M, Hao M, Yang L, Yao H, Bolton JR, Blatchley ER, Qiang Z: Trace organic pollutant removal by VUV/UV/chlorine process: Feasibility investigation for drinking water treatment on a mini-fluidic VUV/UV photoreaction system and a pilot photoreactor. *Environ. Sci. Technol.*, **52**(13), 7426–7433, 2018. PMID:29792423 doi:10.1021/acs.est.8b00611

[105] Wang D, Bolton JR, Hofmann R: Medium pressure UV combined with chlorine advanced oxidation for trichloroethylene destruction in a model water. *Water Res.*, **46**(15), 4677–4686, 2012. PMID:22763292 doi:10.1016/j.watres.2012.06.007

[106] Kedir AJ, Tawabini B, Al-Shaibani A, Bukhari AA: Treatment of water contaminated with methyl tertiary butyl ether using UV/chlorine advanced oxidation process. *Desalination Water Treat.*, **57**(42), 19939–19945, 2016. doi:10.1080/19443994.2015.1106980

[107] Morimoto Y, Sumitomo T, Yoshioka M, Takemura T: Recent progress on UV lamps for industries. Conference Record of the 2004 IEEE Industry Applications Conference, 2004. 39th IAS Annual Meeting, IEEE, pp. 1008–1015, 2004. doi:10.1109/IAS.2004.1348536

[108] Bettles T, Schujman S, Smart JA, Liu W, Schowalter L: UV light emitting diodes − Their applications and benefits. *IUVA News*, **9**(2), 11–15, 2007.

[109] Kwon M, Yoon Y, Kim S, Jung Y, Hwang TM, Kang JW: Removal of sulfamethoxazole, ibuprofen and nitrobenzene by UV and UV/chlorine processes: A comparative evaluation of 275 nm LED-UV and 254 nm LP-UV. *Sci. Total Environ.*, **637-638**, 1351–1357, 2018. PMID:29801227 doi:10.1016/j.scitotenv.2018.05.080

[110] Wang WL, Wu QY, Li ZM, Lu Y, Du Y, Wang T, Huang N, Hu HY: Light-emitting diodes as an emerging UV source for UV/chlorine oxidation: Carbamazepine degradation and toxicity changes. *Chem. Eng. J.*, **310**, 148–156, 2017. doi:10.1016/j.cej.2016.10.097

[111] Iqbal M: The solar constant and its spectral distribution. In: Iqbal M (ed): An Introduction to Solar Radiation, Academic Press, Ontario, Canada, pp. 43–58, 1983. doi:10.1016/B978-0-12-373750-2.50008-2

[112] Izadifard M, Langford CH, Achari G: Alternative view of chlorine oxidation stimulated by longer wavelength light. *J. Environ. Eng.*, **142**(10), 04016048, 2016. doi:10.1061/(ASCE)EE.1943-7870.0001124

[113] Young TR, Li W, Guo A, Korshin GV, Dodd MC: Characterization of disinfection byproduct formation and associated changes to dissolved organic matter during solar photolysis of free available chlorine. *Water Res.*, **146**, 318–327, 2018. PMID:30316167 doi:10.1016/j.watres.2018.09.022

[114] Urey HC, Dawsey LH, Rice FO: The absorption spectrum and decomposition of hydrogen peroxide by light. *J. Am. Chem. Soc.*, **51**(5), 1371–1383, 1929. doi:10.1021/ja01380a011

[115] Dogliotti L, Hayon E: Flash photolysis of per[oxydi]sulfate ions in aqueous solutions. The sulfate and ozonide radical anions. *J. Phys. Chem.*, **71**(8), 2511–2516, 1967. doi:10.1021/j100867a019

[116] Li W, Jain T, Ishida K, Remucal CK, Liu H: A mechanistic understanding of the degradation of trace organic contaminants by UV/hydrogen peroxide, UV/persulfate and UV/free chlorine for water reuse. *Environ. Sci. Water Res. Technol.*, **3**(1), 128–138, 2017. doi:10.1039/C6EW00242K

[117] Guo K, Wu Z, Yan S, Yao B, Song W, Hua Z, Zhang X, Kong X, Li X, Fang J: Comparison of the UV/chlorine and UV/H$_2$O$_2$ processes in the degradation of PPCPs in simulated drinking water and wastewater: Kinetics, radical mechanism and energy requirements. *Water Res.*, **147**, 184–194, 2018. PMID:30312791 doi:10.1016/j.watres.2018.08.048

[118] Varanasi L, Coscarelli E, Khaksari M, Mazzoleni LR, Minakata D: Transformations of dissolved organic matter induced by UV photolysis, Hydroxyl radicals, chlorine radicals, and sulfate radicals in aqueous-phase UV-Based advanced oxidation processes. *Water Res.*, **135**, 22–30, 2018. PMID:29454238 doi:10.1016/j.watres.2018.02.015

[119] Miklos DB, Remy C, Jekel M, Linden KG, Drewes JE, Hübner U: Evaluation of advanced oxidation processes for water and wastewater treatment – A critical review. *Water Res.*, **139**, 118–131, 2018. PMID:29631187 doi:10.1016/j.watres.2018.03.042

[120] Moussallem I, Jörissen J, Kunz U, Pinnow S, Turek T: Chlor-alkali electrolysis with oxygen depolarized cathodes: history, present status and future prospects. *J. Appl. Electrochem.*, **38**(9), 1177–1194, 2008. doi:10.1007/s10800-008-9556-9

[121] de Mello Florêncio T, de Araújo KS, Antonelli R, de Toledo Fornazari AL, da Cunha PCR, da Silva Bontempo LH, de Jesus Motheo A, Granato AC, Malpass GRP: Photo-assisted electrochemical degradation of simulated textile effluent coupled with simultaneous chlorine photolysis. *Environ. Sci. Pollut. Res. Int.*, **23**(19), 19292–19301, 2016. PMID:27364489 doi:10.1007/s11356-016-6912-x

[122] Li J, Blatchley ER III: UV photodegradation of inorganic chloramines. *Environ. Sci. Technol.*, **43**(1), 60–65, 2009. PMID:19209585 doi:10.1021/es8016304

[123] Dodd MC, Zuleeg S, Gunten U, Pronk W: Ozonation of source-separated urine for resource recovery and waste minimization: process modeling, reaction chemistry, and operational considerations. *Environ. Sci. Technol.*, **42**(24), 9329–9337, 2008. PMID:19174912 doi:10.1021/es800560r

[124] Chuang YH, Chen S, Chinn CJ, Mitch WA: Comparing the UV/monochloramine and UV/free chlorine advanced oxidation processes (AOPs) to the UV/hydrogen peroxide AOP under scenarios relevant to potable reuse. *Environ. Sci. Technol.*, **51**(23), 13859–13868, 2017. PMID:29121472 doi:10.1021/acs.est.7b03570

[125] Wang W, Sha J, Lu Z, Shao S, Sun P, Hu Q, Zhang X: Implementation of UV-based advanced oxidation processes in algal medium recycling. *Sci. Total Environ.*, **634**, 243–250, 2018. PMID:29627547 doi:10.1016/j.scitotenv.2018.03.342

[126] Bu L, Zhou S, Zhu S, Wu Y, Duan X, Shi Z, Dionysiou DD: Insight into carbamazepine degradation by UV/monochloramine: Reaction mechanism, oxidation products, and DBPs formation. *Water Res.*, **146**, 288–297, 2018. PMID:30292129 doi:10.1016/j.watres.2018.09.036

[127] Benarde MA, Snow WB, Olivieri VP, Davidson B: Kinetics and mechanism of bacterial disinfection by chlorine dioxide. *Appl. Microbiol.*, **15(2)**, 257-265, 1967. doi:10.1073/pnas.1208755109

[128] Reid PJ: Investigating the phase-dependent reactivity of chlorine dioxide using resonance raman spectroscopy. *J. Phys. Chem. A*, **106**(8), 1473–1482, 2002. doi:10.1021/jp013491y

[129] Wang D, Bolton JR, Andrews SA, Hofmann R: UV/chlorine control of drinking water taste and odour at pilot and full-scale. *Chemosphere*, **136**, 239–244, 2015. PMID:26025188 doi:10.1016/j.chemosphere.2015.05.049

[130] Watts MJ, Hofmann R, Rcdsenfeldt EJ: Low-pressure UV/Cl$_2$ for advanced oxidation of taste and odor. *J. Am. Water Works Assoc.*, **104**(1), E58–E65, 2012. doi:10.5942/jawwa.2012.104.0006

[131] Yang X, Sun J, Fu W, Shang C, Li Y, Chen Y, Gan W, Fang J: PPCP degradation by UV/chlorine treatment and its impact on DBP formation potential in real waters. *Water Res.*, **98**, 309–318, 2016. PMID:27110887 doi:10.1016/j.watres.2016.04.011

[132] Zuo Z, Katsumura Y, Ueda K, Ishigure K: Reactions between some inorganic radicals and oxychlorides studied by pulse radiolysis and laser photolysis. *J. Chem. Soc., Faraday Trans.*, **93**(10), 1885–1891, 1997. doi:10.1039/a700256d

[133] Jayson GG, Parsons BJ, Swallow AJ: Some simple, highly reactive, inorganic chlorine derivatives in aqueous solution. Their formation using pulses of radiation and their role in the mechanism of the Fricke dosimeter. *J. Chem. Soc. Faraday Trans. 1 Phys. Chem. Condens. Phases*, **69**, 1597–1607, 1973. doi:10.1039/F19736901597

[134] Siddiqui MS: Chlorine-ozone interactions: Formation of chlorate. *Water Res.*, **30**(9), 2160–2170, 1996. doi:10.1016/0043-1354(96)00071-1

[135] Buxton GV, Subhani MS: Radiation chemistry and photochemistry of oxychlorine ions. Part 1.—Radiolysis of aqueous solutions of hypochlorite and chlorite ions. *J. Chem. Soc. Faraday Trans. 1 Phys. Chem. Condens. Phases*, **68**, 947–957, 1972. doi:10.1039/f19726800947

[136] Lister MW: Decomposition of sodium hypochlorite: the catalyzed reaction. *Can. J. Chem.*, **34**(4), 479–488, 1956. doi:10.1139/v56-069

[137] Odeh IN, Francisco JS, Margerum DW: New pathways for chlorine dioxide decomposition in basic solution. *Inorg. Chem.*, **41**(24), 6500–6506, 2002. PMID:12444796 doi:10.1021/ic0204676

[138] Quiroga SL, Perissinotti LJ: Reduced mechanism for the 366 nm chlorine dioxide photodecomposition in N$_2$-saturated aqueous solutions. *J. Photochem. Photobiol. Chem.*, **171**(1), 59–67, 2005. doi:10.1016/j.jphotochem.2004.09.006

[139] Buxton GV, Subhani MS: Radiation chemistry and photochemistry of oxychlorine ions. Part 3.—Photodecomposition of aqueous solutions of chlorite ions. *J. Chem. Soc. Faraday Trans. 1 Phys. Chem. Condens. Phases*, **68**, 970–977, 1972. doi:10.1039/f19726800970

[140] Kläning UK, Sehested K: The primary process ClO$_3^-$ (+hv) → ClO$^-$ + O$_2$ in the photolysis of aqueous chlorate solutions. *J. Phys. Chem.*, **95**(2), 740–743, 1991. doi:10.1021/j100155a046

[141] Mansor NA, Tay KS: Degradation of 5,5-diphenylhydantoin by chlorination and UV/chlorination: kinetics, transformation by-products, and toxicity assessment. *Environ. Sci. Pollut. Res. Int.*, **24**(28), 22361–22370, 2017. PMID:28801887 doi:10.1007/s11356-017-9892-6

[142] Zhang X, Li J, Yang JY, Wood KV, Rothwell AP, Li W, Blatchley ER: Chlorine/UV process for decomposition and detoxification of microcystin-LR. *Environ. Sci. Technol.*, **50**(14), 7671–7678, 2016. PMID:27338715 doi:10.1021/acs.est.6b02009

[143] Boal AK, Rhodes C, Garcia S: Pump-and-treat groundwater remediation using chlorine/ultraviolet advanced oxidation processes. *Ground Water Monit. Remediat.*, **35**(2), 93–100, 2015. doi:10.1111/gwmr.12095

[144] Nam SW, Yoon Y, Chae S, Kang JH, Zoh KD: Removal of Selected Micropollutants During Conventional and Advanced Water Treatment Processes. *Environ. Eng. Sci.*, **34**(10), 752–761, 2017. doi:10.1089/ees.2016.0447

[145] Pati SG, Arnold WA: Reaction rates and product formation during advanced oxidation of ionic liquid cations by UV/peroxide, UV/persulfate, and UV/chlorine. *Environ. Sci. Water Res. Technol.*, **4**(9), 1310–1320, 2018. doi:10.1039/C8EW00254A